Published in final edited form as:
*Lipids*. 2008 December ; 43(12): 1185–1208. doi:10.1007/s11745-008-3194-1.

# Fluorescence Techniques Using Dehydroergosterol to Study Cholesterol Trafficking

**Avery L. McIntosh**[@], **Barbara P. Atshaves**[@], **Huan Huang**[@], **Adalberto M. Gallegos**[#], **Ann B. Kier**[#], and **Friedhelm Schroeder**[@,*]

# *Department of Pathobiology Texas A&M University, TVMC College Station, TX 77843-4467*

@ *Department of Physiology and Pharmacology Texas A&M University, TVMC College Station, TX 77843-4466*

## Abstract

Cholesterol itself has very few structural/chemical features suitable for real-time imaging in living cells. Thus, the advent of dehydroergosterol [ergosta-5,7,9(11),22-tetraen-3β-ol, DHE] the fluorescent sterol most structurally and functionally similar to cholesterol to date, has proven to be a major asset for real-time probing/elucidating the sterol environment and intracellular sterol trafficking in living organisms. DHE is a naturally-occurring, fluorescent sterol analog that faithfully mimics many of the properties of cholesterol. Because these properties are very sensitive to sterol structure and degradation, such studies require the use of extremely pure (>98%) quantities of fluorescent sterol. DHE is readily bound by cholesterol-binding proteins, is incorporated into lipoproteins (from the diet of animals or by exchange *in vitro*), and for real-time imaging studies is easily incorporated into cultured cells where it co-distributes with endogenous sterol. Incorporation from an ethanolic stock solution to cell culture media is effective, but this process forms an aqueous dispersion of dehydroergosterol crystals which can result in endocytic cellular uptake and distribution into lysosomes which is problematic in imaging DHE at the plasma membrane of living cells. In contrast, monomeric DHE can be incorporated from unilamellar vesicles by exchange/fusion with the plasma membrane or from DHE-methyl-β-cyclodextrin (DHE-MβCD) complexes by exchange with the plasma membrane. Both of the latter techniques can deliver large quantities of monomeric dehydroergosterol with significant distribution into the plasma membrane. The properties and behavior of DHE in protein-binding, lipoproteins, model membranes, biological membranes, lipid rafts/caveolae, and real-time imaging in living cells indicate that this naturally-occurring fluorescent sterol is a useful mimic for probing the properties of cholesterol in these systems.

### Keywords

dehydroergosterol; cholesterol; ergosterol; fluorescent sterols; microscopy

## 1. Historical Perspective

In order to resolve the dynamics and factors governing cholesterol trafficking within cells, it is important to recognize that the cholesterol molecule has very few polar constituents (Fig. 1A). Consequently, cholesterol is poorly soluble in aqueous environments such as cytosol as evidenced by critical micellar concentrations of cholesterol and other sterols being very low,

*To whom correspondence should be addressed: Department of Physiology and Pharmacology, Texas A&M University, TVMC, College Station, TX 77843-4466. Phone: (979) 862-1433, FAX: (979) 862-4929, E-mail: FSchroeder@cvm.tamu.edu.

near 20–30 nM (1–5). The physiological impact of cholesterol's low aqueous solubility is that spontaneous cholesterol desorption from the cytofacial leaflet of the plasma membrane or lysosomal membrane into the cytosol for transfer to intracellular sites for esterification, oxidation, or secretion is extremely slow ($t_{1/2}$ 3 hours-days) (6–9). Therefore, it is important to resolve factors that influence the solubility of cholesterol in the cytoplasm as well as to understand how the architecture and properties of cholesterol in the plasma membrane govern cholesterol movement from serum lipoproteins/albumin into the membrane exofacial leaflet, across the bilayer, and from the membrane cytofacial leaflet into the cytoplasm either as vesicles or to cholesterol binding proteins.

Multiple physical approaches in model or fixed cell systems have been used to resolve the properties of cholesterol in membranes and the influence of cholesterol on membrane structure. Membrane cholesterol organization has been examined using electron microscopy to visualize the membrane at magnifications up to 100,000X (10). X-ray diffraction has been applied to membranes to determine cholesterol orientation and depth as well as determine lipidic crystal structures (11,12). By using deuterated molecules and cooled neutron beams, neutron scattering profiles of phospholipid/cholesterol bilayers have been measured and neutron scatter off of the deuterium atom has been used to accurately determine cholesterol's location within the membrane (11,12). Electron scattering has had limited use due to high vacuum requirements but has yielded some packing orientation of cholesterol-rich domains (11–13). Calorimetry or thermal analysis resolves the effects of cholesterol level on lipid phase transitions in model membranes of various lipid compositions (14). Unfortunately the complexity of lipid compositions in biological membranes broadens/abolishes lipid phase transitions—thereby limiting the usefulness of calorimetry. By placing the membranes in a strong magnetic field with exposure to electromagnetic radiation, nuclear magnetic resonance (NMR) measurements involving the interaction with the nonzero spin of certain nuclei such as $^{1}H$ and $^{13}C$ have provided not only detailed structural information (*e.g.* order parameter) on cholesterol but also its interaction strengths with phospholipid constituents of the membrane (12,15,16). While $^{1}H$ and $^{13}C$ labeled cholesterols provide probes with structure most closely resembling that of cholesterol, it is difficult to incorporate large amounts of these labeled sterols into biological membranes and the time-scale of NMR measurements precludes resolution of cholesterol dynamics on the biological time-scale (17). Another technique, electron spin resonance (EPR) involves the exploitation of the paramagnetism of certain molecules with unpaired spins, usually $^{14}N$ (15). Due to the nature of the low natural paramagnetism of lipids, EPR probes are synthesized with spin labels such as nitroxide free radicals (*e.g.* dimethyl nitroxide referred to as doxyl). The properties of doxyl labeled sterol analogs such as SL-cholestane, SL-cholesterol, and SL-androstane have recently been examined in POPC large unilamellar vesicles (LUVs). Using EPR, it was found that the SL-cholestane was moved deeper within the membrane as a result of the bulky doxyl replacing the OH group but with correct membrane orientation similar to the SL-cholesterol which had the doxyl replacing two methyl groups in the cholesterol tail (16). However, EPR showed that the SL-androstane molecule was upside down in membrane orientation. This was due to the hydroxyl at the terminal end of the lipid chain and the replacement of the OH by the doxyl group (16). Other techniques to examine cholesterol architecture in membranes have included radiolabeled methods, Raman scattering, and absorption techniques including infrared and optical rotation dispersion/circular dichroism. While these approaches have been very useful for studies of model membrane systems, purified biological membrane fractions *in vitro*, or membranes of fixed cells, they have not provided much insight into cholesterol dynamics in living cells.

Obviously, a great deal of effort has been made to design both suitable cholesterol analogs and the respective experimental methods to gain insights into the lipid domain structure and dynamics of biological membranes. Nevertheless, there is concern whether the behavior of the cholesterol analogues truly reflects that of cholesterol. Most of the probes have been chosen

for the respective studies based on their close structural and organizational resemblance to the cholesterol molecule in both natural and artifical membranes. Until recently it was almost universally accepted that cholesterol represents the unique and essential building block of the cell membrane which defines, to a great extent, the normal function of biological organisms including man and most animals. Under this paradigm even small alterations in the chemical structure of cholesterol would be predicted to be incompatible with animal life (rev. in (18). But is cholesterol really essential for normal cell organization and function? How stringent are the stereo- and physico-chemical criteria for the membrane sterol molecule that creates a platform (environment) for membrane proteins? Several studies suggest that many aspects of the original paradigm—i.e. compatibility with life—may be met by sterols other than cholesterol: (i) Simple animal cells such as yeast (*Candida tropicalis*, *Saccharomyces cerevisiae*) and Red Sea sponge (*Biemna fortis*) synthesize DHE (Fig. 1A) as a major membrane sterol component (19–21). DHE differs from cholesterol by having an ergosterol side-chain (i.e. branched methyl and double bond), an ergosterol B ring (two double bonds), and a C ring with an additional double bond that maintains the extended cyclopentanophenanthrene ring structure (Fig. 1A); (ii). DHE completely replaces the requirement for cholesterol as the only sterol source in the diet of the worm *C. elegans* (19); (iii) Mouse L-cell fibroblasts lack the enzyme 3β-hydroxysteroid-$\Delta^{24}$-reductase (desmosterol reductase, Dhcr24) (22). Desmosterol differs from cholesterol in having an extra double bound in the side chain. When cultured in chemically-defined medium the L-cells synthesize desmosterol, replace membrane cholesterol with desmosterol, and grow normally despite the absence of cholesterol (22,23); (iv). Mouse L-cells cultured in chemically-defined medium containing dehydroergosterol (DHE) accumulate DHE which replaces as much as 90% of endogenous membrane sterol without adverse effects on membrane phospholipid or fatty acid composition, sterol/phospholipid ratio, activity of cholesterol sensitive enzymes in the plasma membrane, or cell growth (24). Similar observations have been made with cultured human fibroblasts and MDCK cells (25–27); (v). Most of the cholesterol in the developing and early neonatal rat retina can be replaced by desmosterol without alteration in function (28); (v) Ablation of the enzyme 3β-hydroxysteroid-$\Delta^{24}$-reductase (desmosterol reductase, Dhcr24) in mice is not lethal and such mice exhibit only a mildly altered phenotype evidenced by disturbances occurring in steroid homeostasis (18, 29). The development of these viable “cholesterol-free mice”, where almost all of the cholesterol is replaced by desmosterol, shows that there is not an absolute requirement for cholesterol to maintain life (18,29). It should be noted, however, that the same mutation in humans causes severe abnormalities, likely due to the inability of human embryos to access maternal cholesterol which is in contrast to mouse embryogenesis where maternal cholesterol is available (18). Taken together, these data suggest that the membranes of mammalian and other animal cells can tolerate small changes in the structure of the cholesterol side (desmosterol, DHE) and ring structure (DHE) and remain viable. However, not all small changes in the cholesterol structure are equally well tolerated. For example, loss of the Dhcr7 gene in mice (Smith-Lemli-Opitz syndrome in humans) results in accumulation of 7-dehydrocholesterol and very short-lived mice (rev. in (29). Much further work needs to be done to establish the exact substitutions/changes in cholesterol structure that can be accommodated to maintain viability.

## 2. Advent of fluorescent sterols

More recently fluorescence detection has been widely used to study cholesterol not only *in vitro*, but also in real-time imaging of fluorescent sterols (Fig. 1B-F) in living cultured cells or *in vivo*. Fluorescent sterols, like other fluorescent probes, provide ease of handling with very high level sensitivity of detection, relatively short detection times, and multiplexing of several probes (17). These characteristics of fluorescence detection have made it very beneficial in utilizing small quantities of fluorescent sterols not only for use with traditional spectrofluorometers but also in newly developed systems. In particular, fluorescent sterols and

other probes have brought about the widespread use of laser scanning confocal microscopy (LSCM) and multiphoton laser scanning microscopy (MPLSM) to simultaneously study the interaction of lipids like cholesterol and proteins/receptors in real-time within living cells.

With rare exception, the fluorophores present in most commercially available fluorescent sterol (Avanti Polar Lipids, Alabaster, AL; Invitrogen, Carlsbad, CA; Sigma, St. Louis, MO) as well as those synthesized in individual laboratories are synthetic chemical tags that have been used to localize cholesterol in membranes. This includes the weakly fluorescent photoactivatable free cholesterol benzophenone FCBP that photocross-links to proteins or lipids (Fig. 1B), the cholesterol-rich microdomain preferring cholesterol analogs such as Dansyl-cholesterol (6-Dansyl-cholestanol) and BODIPY-cholesterol analog LZ260 (Fig. 1C), and the cholesterol-poor microdomain preferring BODIPY-coprostanol, BODIPY-cholesterol analog LZ110a, 22-NBD-cholesterol (Fig. 1D), 25-NBD-cholesterol (not shown), etc. (16,30–38). Although there is considerable discussion regarding the solubility and orientation of these synthetic fluorescent sterol probes in membrane bilayers, especially 22-NBD-cholesterol and 25-NBD-cholesterol, at low concentrations some are thought to mimic the distribution and orientation of cholesterol (16,35–37). However, relatively few have been examined with regards to their ability to be bound by intracellular cholesterol-binding proteins (*e.g.* SCP-2, ADRP) or their real-time uptake, distribution, and efflux dynamics in living cells. One exception is 22-NBD-cholesterol which has been shown to be not only bound with high affinity (nM $K_d$s) by SCP-2 and ADRP, but with orientation within the binding site similar to cholesterol—suggesting that this probe may be suitable for study of intracellular cholesterol trafficking (4,39–44). Indeed, 22-NBD-cholesterol has proven useful for real-time imaging of HDL-mediated cholesterol uptake, efflux, and intracellular trafficking in living cells such as L-cell fibroblasts as well as rat macrophages and lymphocytes (43,45,46). Sterol carrier protein-2 (SCP-2) overexpression facilitated (*i.e.* decreased $t_{1/2}$ of efflux) of protein mediated NBD-cholesterol cytosolic efflux (43). Concomitantly SCP-2 overexpression decreased the slower, vesicular cholesterol transfer —likely by binding and sequestering ligands (i.e. phosphatidylinositides, fatty acyl CoAs) that regulate vesicular trafficking (43,47–53).

However, there is a small group of naturally fluorescent lipids that includes sterols such as dehydroergosterol (DHE, Fig. 1A) as well as some fatty acids (parinaric acids), retinoids (retinol, retinoic acid), carotenes, and steroids (estriol). Because of the tremendous interest of biologists and membraneologists in cholesterol-rich microdomains (also called lipid rafts or caveolae) over the past 15 years (rev. in (54–63), DHE has emerged as a popular, potentially less perturbing fluorescent sterol probe since it does not contain additional bulky fluorescent groups added to the sterol structure. Although this ultraviolet (UV) light absorbing and fluorescent sterol (*i.e.* DHE) was first chemically synthesized over 50 years ago (64), it was its detection at high level in membranes of eukaryotes such as yeast *Candida tropicalis* (19) and Red Sea sponge *Biemna fortis* (21) that suggested its potential usefulness as a probe for cholesterol. Consequently, the focus of the remainder of the current review is on the use of naturally fluorescent DHE as a probe of cholesterol behavior in sterol-protein interactions, lipoproteins, model membranes, biological membranes, and lipid rafts/caveolae. Since cholesterol itself has very few structural/chemical features suitable for UV/VIS or optical imaging, the advent of DHE with many properties mimicking or very similar to those of cholesterol, has proven to be a major asset for probing/elucidating real-time sterol dynamics by video and MPLSM imaging in living cells. For additional insights, the reader is referred to earlier reviews on DHE, synthetic fluorescent sterols, spin labeled sterols, photoreactive sterols, and chemical tags of cholesterol (65–68).

## 3. Effect of Sterol Structure and Purity on Sterol Architecture and Dynamics in Membranes

Despite the fact that DHE is a naturally occurring fluorescent sterol appearing in sponge and yeast, it is not generally obtained from these sources. Instead, DHE from commercial (Sigma, St. Louis, MO) as well as laboratory sources is chemically synthesized by an adaptation of a 50 year old method (64,69–71). However, synthetic DHE prepared by this established method, especially that obtained from commercial sources, may contain a significant sterol impurity, varying from batch to batch, and as high as 20–40% (43,70,71). It is important to note that not only the quantity, but also the chemical structure of the sterol and the presence of cholesterol oxidation products are known to significantly affect the structure and/or function of model membranes (rev. in (54,55,70,72,73), biological membranes (13,74–80), lipid raft/caveolae (58,81–88), and cholesterol-requiring plasma membrane receptors (66,89–91). Because of this sensitivity it is essential that fluorescent sterols such as DHE not contain other sterols (*e.g.* ergosterol starting material or side products produced during DHE synthesis) or oxidation products. Such sterols/oxidation products may be non-fluorescent, potentially toxic (*e.g.* oxidized sterols), alter membrane structure, and/or not faithfully reflect the properties of cholesterol as accurately as pure DHE. This is even more important for real-time imaging of fluorescent DHE in living cells where such impurities may compete with DHE for uptake and/or may be toxic. Therefore, the following text deals with procedures for removing unreacted substrate (ergosterol), identifying side reaction or oxidation products, removing impurities, and modifying the synthesis procedure to prevent these artifacts. The DHE synthesis procedures described below tested ergosterol substrate obtained from several manufacturers (Steraloids, Wilmington, NH; Aldrich Chemical Co., Milwaukee, WI; Fluka Chemie, Steinheim, Switzerland; Sigma Chemical, St Louis, Mo), but all other reagents were in common from the same manufacturer: “Purified Plus” methanol, chloroform, and ethyl ether were from Burdick-Jackson (Muskegon, MI); “Baker Analyzed” 99$^{+}$% pure glacial acetic acid was from Mallinckrodt Baker (Phillipsburg, NJ), 99$^{+}$% pure acetic anhydride was from VWR (Atlanta, GA), and anhydrous mercuric acetate was from Fisher Scientific (Pittsburgh, PA).

### 3.1. Identification of potential impurities obtained through the classical DHE synthesis procedure

DHE was synthesized from ergosterol by a classical procedure established over 50 years ago (64,69). Purity of DHE was determined by high performance liquid chromatography as described (69). The HPLC elution profile was monitored as follows: absorbance at 205 nm (all constituents), absorbance at 325 nm (DHE), and fluorescence emission at 375 nm (DHE). When the elution profile of commercially available DHE was monitored at 205 nm absorbance, at least two major peaks were obtained with retention times of 11.75 min and 15.3 min, respectively (Fig. 2A). The latter peak comprised at least 20% of total sterol To determine which of these peaks represented DHE, the elution profile was monitored by absorbance at 325 nm (Fig. 2B) and fluorescence emission at 375 nm (Fig. 2C). Only the larger peak near 11.75 min absorbed at 325 nm (Fig. 2B) and fluoresced (Fig. 2C). The smaller peak at 15.3 min comprising about 20% of total sterol was not DHE since it did not absorb or fluoresce at wavelengths typical of DHE. HPLC chromatograms (not shown) of DHE prepared by our laboratory from only one lot of ergosterol (Steraloids), but not from subsequent lots from the same or other sources, yielded pure DHE (>99%). All other preparations yielded DHE which was highly (20–40%) impure. To further resolve the impurity, complete absorbance spectra were obtained. The absorption spectrum of >99% pure DHE showed maxima at 310, 325 nm, and 342 nm (Fig. 3A). In contrast, absorbance spectra of impure synthetic DHE exhibited several additional peaks at 235, 242, and 251 nm (Fig. 3B), more clearly revealed by a difference spectrum (Fig. 3C). The latter absorbance maxima were not consistent with the starting material, ergosterol, which exhibited absorption maxima at much longer wavelengths

271, 281, and 293 nm (not shown). It is important to note that HPLC elution profiles, whether monitored at 205 nm or 242 nm (wavelength at which the impurity absorption was highest), were unable to clearly distinguish whether the impurity was unreacted ergosterol or an as yet unidentified compound with similar retention time (not shown). While mass spectra of the impure DHE detected DHE at $(M+1)^+$ of 395.3 and $(M-OH)^+$ of 377.5 as expected (Fig. 4A), an additional component appeared with $(M+1)^+$ of 397.3 and $(M-OH)^+$ of 379.3 (Fig. 4A). Surprisingly the APCI mass spectrum of this additional component was identical to that of ergosterol (Fig. 4B)—suggesting that the impurity was possibly an isomer of ergosterol. Indeed it was reported nearly 60 years ago that small amounts of nitric acid or mercuric nitrate catalyze not only the formation of the tetraene DHE but also a side product, *i.e.*, mercurated triene, of ergosterol due to double bond rearrangement (92,93). The spectral characteristics (*i.e.*, maxima at 235, 242, and 251 nm) of the DHE impurity were the same as those of an isomer of ergosterol (5,7,22-cholestatrien-24β-methyl-3β-ol ) known as ergosterol D (64,94). Ergosterol D is a triene [*i.e.* (7,9(11),22-cholestatrien-24β-methyl-3β-ol)] which differs from ergosterol (*i.e.* 5,7,22-cholestatrien-24β-methyl-3β-ol) in that the double bonds in the B ring are each displaced one carbon atom position.

Based on the above data, a general scheme of DHE synthesis and formation of the ergosterol D isomer was established (Fig. 5). This scheme suggests that the synthesis of pure DHE involved steps I, II (but *not* IIA), and III (Fig. 5). The presence of some as yet unknown factor ("impurity") in starting material ergosterol, however, resulted in rearrangement in the double bonds in the B ring of ergosterol (essentially a competing side reaction) as shown in step IIA (Fig. 5). This side reaction product was an isomer of ergosterol, ergosterol D [*i.e.* (7,9,22-cholestatrien-24β-methyl-3β-ol)] distinct from the original ergosterol (5,7,22-cholestatrien-24β-methyl-3β-ol) and DHE. In further support of this scheme, the absorbance spectrum of each product during DHE was monitored (Fig.5). The UV absorbance spectrum of ergosterol acetate (step I, Fig. 5) exhibited three absorption maxima (Fig. 3D) essentially identical to pure ergosterol (not shown). Hence, ergosterol acetate formation did not alter UV absorbance spectrum of ergosterol. In Fig. 3E is shown the UV absorbance spectrum of the intermediate product taken 16 h into the 18 h dehydration step (step II, Fig. 5). This spectrum was broad with vibrational bands that were no longer distinct (cf. Fig. 3D). Fig. 3F clearly showed that during formation of DHE acetate (step II in Fig. 5), the side reaction product ergosterol D acetate (step IIA in Fig. 5) was concomitantly formed. Finally, saponification (step III, Fig. 5) of the DHE acetate and the ergosterol D acetate and recrystallization resulted in a UV absorbance spectrum (Fig. 3F) consistent with presence of both DHE (longer wavelength peaks) and ergosterol D (peaks between 230 and 260 nm) as indicated.

### 3.2. Removal of impurities from DHE: Modified DHE synthesis procedure

The fact that HPLC, absorbance spectra, and mass spectral analysis did not detect any other organic contaminant in ergosterol starting material suggested that a water soluble inorganic contaminant might be a contributing factor to the formation of the non-fluorescent ergosterol D side reaction product. Therefore, in an effort to remove potential water-soluble contaminants, the ergosterol was dissolved in chloroform, washed at least three times with an equal amount of deionized water, dried under $N_2$, dissolved in hot methanol and recrystallized three times, and then dried under $N_2$. HPLC analysis to detect all constituents (absorbance at 205) revealed only a single peak was detectable, retention time 11.7 min (Fig. 2D). Likewise, when DHE was specifically monitored by absorbance at 325 nm (Fig. 2E) and fluorescence emission at 375 nm (Fig. 2F) in each case only a single peak was detectable, again with retention time of 11.7 min. HPLC chromatograms and absorbance spectra indicated that DHE synthesized by the modified method was ≥99% pure. Furthermore, APCI mass spectroscopy detected only a single peak with >99% (not shown).

## 4. Monomeric *vs* Crystalline DHE

Many of the spectroscopic properties of DHE as a fluorescent sterol probe have been elucidated in organic solvents (64,65,95) and in aqueous buffers (69,70,96). In organic solvents such as ethanol, DHE exhibits three UV excitation maxima (311, 324, and 340 nm) and three red-shifted emission maxima (354, 371, and 390 nm) characteristic of the DHE monomer. Interestingly, however, in aqueous buffers DHE exhibits a prominent spectral enhancement of the emission maxima near 404 nm and 426 nm as a possible result of excimeric emission—reflecting DHE in microcrystalline structures, but with only a slight (about 5 nm) red shift in both absorbance maxima and emission maxima (70). For instance, the respective excitation and emission maxima at 324 nm and 370 nm in ethanol shifted to 329 nm and 375 nm in aqueous such that the difference in the similar vibronic levels was maintained at 46 nm. This was consistent with solvent polarity (*i.e* dielectric constant) or pH having only a very minor effect on DHE and that charge separation does not occur. Many different organic solvents were used in a previous study to show that the Stokes shift varied between 3867 $cm^{-1}$ and 4000 $cm^{-1}$ (95). The DHE excitation and emission of the aqueous dispersion was similar to spectra of DHE polycrystalline powder; and both forms also exhibited similar lifetimes and corresponding fractions in a dual lifetime analysis (96).

Advantage has been taken of the distinction in the spectral characteristics to differentiate monomeric and microcrystalline (mostly in lysosomes) forms of DHE in living cells visualized by multiphoton imaging (70). In order to determine quantitatively the amount of the crystalline component and monomeric, the DHE was examined by fluorescence spectroscopy wherein the ratio of fluorescence intensity measurements at the wavelengths 426 nm and 373 nm was computed. Under monomeric conditions, such as the case in an organic solvent (*e.g.* ethanol) or low concentrations of DHE in model membranes (*e.g.* large unilamellar vesicles or LUVs), the ratio was measured as $I_{426}/I_{373}$ ~0.3 and would increase to approximately $I_{426}/I_{373}$ ~3.4 for an aqueous dispersion of DHE in a buffered solution with pH. 7.4 (70). Thus, the spectral properties of DHE give important insights on the cholesterol organization in membranes or organelles (*e.g.* lysosomes).

## 5. DHE Properties in Lipoproteins, Cholesterol-Binding Proteins, and Peptides

DHE has been directly incorporated into lipoproteins *in vitro* (97–99) or *in vivo* by feeding animals (rats, rabbits) dietary DHE followed by isolation of serum lipoproteins (100,101). These studies showed that DHE was localized in the surface monolayer surrounding the neutral lipid cores of triglyceride/cholesteryl ester rich lipoproteins similarly as cholesterol. In addition, DHE and a similar synthetic fluorescent cholesterol analog (cholestatrienol, CTE) have been used to examine the structure of the sterol binding site of cholesterol-binding proteins such as sterol carrier protein-2 (SCP-2) (2,39,102–105) and liver fatty acid binding protein (L-FABP) (2,106,107). SCP-2 and L-FABP generally bound one mole of fluorescent sterol/mole protein. The fluorescent DHE or CTE were highly ordered in the binding pockets as indicated by markedly increased polarization as compared to aqueous buffer. The intermolecular distance between the DHE or CTE fluorophore and Trp or Tyr residues of these proteins measured by a fluorescence resonance energy transfer (FRET) in these studies was in the range of 16–19 Å, indicating close molecular interaction (108). Finally, FRET between Trp of mellitin (peptide from bee venom) and DHE incorporated in model membranes indicated that mellitin bound to the membrane, bound mellitin Trp was in close proximity to DHE (*i.e.* a few angstroms), and DHE was non-randomly distributed within the model membrane (109). Taken together these findings were consistent with DHE as a useful probe for examining the interactions and location of cholesterol in cholesterol-binding proteins and lipoproteins.

# 6. DHE Properties in Membranes

## 6.1. Model Membranes

The usefulness of DHE and cholestatrienol (CTE) as fluorescent cholesterol analogs in model membranes in a series of investigations spanning several decades demonstrated the usefulness of these probes to monitor cholesterol structural (polarization, limiting anisotropy, order) and dynamic (lifetime, rotational rate) properties in membranes (12,65,70,95,96,108,110–120). The lifetime studies resolved for the first time at least two DHE domains in model membranes, one less sensitive to the aqueous than the other, and that these domains were dependent on the lipid composition, temperature, and other properties of the membrane (54,119). This possibility was further supported by model membrane studies of DHE exchange which provided kinetic evidence for the existence of multiple sterol containing domains in membranes (118,121–124). DHE was especially useful for these studies because the spontaneous exchange of DHE between model membranes was very similar to that of radiolabeled cholesterol (117). Further, these dynamic and kinetic pools of DHE represent lateral sterol-rich and –poor domains rather than pools in the outer *vs.* inner leaflet because: (i) the transbilayer distribution of sterol across model membrane bilayers is uniform, unless membranes are very highly curved (rev. in (12)), (ii) the transbilayer migration rate of DHE is very rapid (much faster than kinetic exchange rates between membranes) and is very similar to that of cholesterol (108), (iii) Dynamic (lifetime) and DHE kinetic exchange studies determined that the presence of a large and a small DHE pool, (iv) DHE kinetic exchange studies determined that the large sterol pool corresponded to very-slowly (days) exchangeable sterol, while the small pool (generally <10%) was rapidly exchangeable. The pool size and half-times of exchange were dramatically affected by the presence of acidic phospholipids and, even more so by the presence of sphingolipids in the model membranes. The sterol carrier protein SCP-2 rapidly facilitated DHE transfer between model membranes by decreasing the half-time of exchange and increasing the size of the rapidly exchangeable domain. This action of SCP-2 was mechanistically due not only to the presence of a sterol binding site in this protein, but also the membrane interaction domain comprised on a positively charged face of an N-terminal amphipathic α-helix (125–127). These studies demonstrated that the properties of DHE and/or CTE closely reflected those of cholesterol in model membranes.

## 6.2 Suitability of DHE as a Probe for Cholesterol in Biological Membranes

DHE is non-toxic to animal cells as shown by its presence in membranes of yeast (*Candida tropicalis*, *Saccharomyces cerevisiae*) and Red Sea sponge (*Biemna fortis*) as well as its ability to completely replace cholesterol as the only sterol source in the diet of animals such as *C. elegans* or cultured L-cells (19–21,24,128). Unlike most synthetic fluorescent tagged sterols which can only be incorporated at very low amounts into cell membranes, DHE taken up by cultured cells can replace nearly 90% of total cholesterol without adverse effect on cell viability, plasma membrane structure, plasma membrane phospholipid composition or sterol/phospholipid ratio, or plasma membrane sterol sensitive enzymes (24). Plasma membrane receptors such as the oxytocin receptor are exquisitely sensitive to the structure of the sterol with which it interacts. In cholesterol-depleted membranes, only cholesterol and DHE are effective in reconstituting activity of this highly sterol-sensitive plasma membrane protein (89–91). In cultured cells DHE codistributes with cholesterol in plasma membranes, microsomes, mitochondria, and lysosomes (24,129,130).

## 6.3 Delivery of DHE into Cultured Cell Membranes

DHE may be delivered to living cells for uptake and incorporation into plasma membranes by several methods: (i) While relatively slow, the simplest is *delivery as micro-crystalline DHE* from a stock solution in ethanol over a 2 day period as described previously (24,70). DHE can enter the cells by exchange between the micro-crystals and the cell surface plasma membrane,

a process that may be facilitated by albumin in the medium (131–134). Concomitantly, the cultured cells also phagocytose DHE micro-crystals from the medium as shown by MPLSM colocalization with lysosomal markers (70). Over time the endocytosed DHE micro-crystals may be digested/disrupted in the lysosome or outside the lysosome by intracellular cholesterol-binding proteins such as SCP-2. Consequently, most DHE delivered in this fashion is codistributed similarly as cholesterol in all subcellular membranes including plasma membranes, plasma membrane cholesterol-rich lipid rafts, plasma membrane cholesterol-poor non-rafts, lysosomes, endoplasmic reticulum, and mitochondria (6,7,24,26,27,129,135–137). The presence of DHE micro-crystals in MPLSM images of cells cultured with DHE micro-crystals can be reduced by pulse labeling the cells with DHE micro-crystals for several hours followed by washing and incubation in DHE free medium for several days. (ii) An even slower, but more physiological method is to *deliver DHE complexed to serum lipoproteins* (100, 101). In this method the DHE is dissolved in organic solvent which is used to coat the inside of a tube or (to increase surface area) a tube containing celite (diatomaceous earth), the solvent is evaporated, serum lipoproteins are added in buffer with antimicrobial agent, incubated overnight with shaking at 37°C, followed by sedimentation to remove particulates and filtration to assure sterility. (iii) A faster, but less efficient method to *deliver DHE as a component of large unilamellar vesicles (LUVs)* over a 1 day period as described previously (70). The DHE present in the LUVs enters the cell either by exchange with the cell plasma membrane (potentially facilitated by albumin in the medium) or, depending on the charge of the LUV, by facilitated fusion with the cell plasma membrane. While the LUV method completely avoids the presence of micro-crystalline DHE, less total DHE is incorporated into the cells since incubation with larger amounts of LUVs concomitantly results in incorporation large amounts of carrier phospholipid which itself may alter cell membrane properties depending on the specific phospholipid polar head group (e.g. choline, ethanolamine, etc) and esterified fatty acids (saturated, monounsaturated, polyunsaturated). (iv) The most rapid method for delivery of large amounts of DHE into cells is to *deliver DHE as dehydroergosterol-methyl-β-cyclodextrin (DHE-MβCD) complexes* prepared by adding DHE to an aqueous solution of MβCD (3mM DHE and 30mM MβCD). This mixture was overlaid with $N_2$, continuously vortexed under light protection for 24 h at room temperature, and filtered through a 0.2 μm filter to remove insoluble material and DHE crystals. Then, 20 μg of DHE was added to the cells in the form of DHE-MβCD complexes and allowed to incubate for 45 minutes at room temperature in PBS. Prior to imaging, cells were washed three times with PBS. With this technique DHE enters the cell by exchange between the DHE-MβCD complexes and the cell plasma membrane. The cyclodextrin-based method for DHE delivery to the cell may proceed, in addition to the clathrin mediated pathway, through the caveolae-dependent endocytosis due to non-selective cholesterol loading onto the plasma membrane by cyclodextrin. The major drawback of this method is that large excess of MβCD by itself can deplete cells of cholesterol while very high quantities of DHE-MβCD at high molar ratios can increase total sterol content. Therefore, care must be taken to optimize the DHE-MβCD molar ratio and concentration in the medium to maintain unaltered total sterol content in the cell and cell membranes.

In summary, the above methods of DHE delivery differ in rapidity, the amount of DHE that can be delivered, and potentially DHE distribution in the cell may differ from one loading method or another. The latter may be an advantage of a particular method if it is desirable to preferentially label a specific cellular compartment. Alternately, if uniform distribution of DHE is desired, this potential problem may be minimized if the cells are incubated over sufficient time for the DHE to equilibrate between all cellular compartments.

### 6.4 DHE Architecture in Purified Biological Membranes

DHE has been used to probe the structural (polarization, limiting anisotropy, order), dynamic (lifetime, rotational rate), and kinetic (exchange) environment of cholesterol in plasma

membranes (6,7,54,55,135,138–141), microsomes (6,7), mitochondria (6,7,142,143), and lysosomes (8,129). DHE has revealed several important structural and dynamic aspects of the cholesterol microenvironment in biological membranes.

First, in contrast to model membranes, DHE was found to be asymmetrically distributed across the plasma membrane bilayer (rev. in (12,144,145). DHE revealed that the cytofacial leaflet of plasma membranes from L-cell fibroblasts (12,24,146,147), erythrocytes (144), and brain synaptosomes (145,148–151). While other methods (filipin staining, exchange, cholesterol oxidase accessibility, neutron diffraction, etc) have also been used to measure transbilayer cholesterol distribution, many have significant limitations including accessibility of membrane cholesterol (filipin, cholesterol oxidase), production of a potential perturbant (cholesterol oxidase produces cholesterone), and poor dynamic resolution (neutron diffraction) (rev. in (12). While measurements of transbilayer sterol distribution by different methods may therefore not necessarily agree, multiple methods (DHE, NBD-cholesterol quenching, and exchange assays) indicate that the cytofacial leaflet of erythrocytes has more cholesterol than the exofacial leaflet (144,152). Likewise, several methods (DHE, cholesterol oxidase) indicate that the synaptosomal plasma membrane has more cholesterol in the cytofacial leaflet than the exofacial leaflet (12,145,148–150). The transbilayer distribution of sterol is a major determinant of the transbilayer fluidity gradient present in these membranes, the cytofacial cholesterol-rich leaflet is more rigid (less fluid) than the relatively cholesterol-poor exofacial leaflet (rev. in (146,147,149,153–159). The transbilayer migration rate of DHE in model membranes and plasma membranes is relatively fast, $t_{1/2}$ of sec-min depending on the membrane examined (rev. in (12,108,144,145). Rapid transbilayer migration of DHE is also supported by the finding that uptake of DHE into and non-vesicular transport across cultured hepatocyte-derived cells (i.e. from basolateral to canalicular plasma membrane) is also very rapid, i.e. $t_{1/2}$ of 1–3 min (160). The finding of rapid transbilayer sterol movement suggested that the asymmetric transbilayer distribution in the plasma membrane was not due to restricted movement of cholesterol from one leaflet to the other, but was instead a property of the lipid bilayer itself. DHE transbilayer distribution has broad applicability in studies of the action of anesthetics, cholesterol lowering drugs (statins), alcohol (chronic and acute), lupus erythematosus, aging, apoE, and sterol carrier proteins all of which can alter plasma membrane or synaptosomal plasma membrane transbilayer sterol distribution and/or transbilayer fluidity (26,135,136,145,149,150,154,161–172).

Second, the DHE lateral distribution in both model and biological membranes was not uniform, but instead reflected sterol-rich and poor domains (rev. in (54,55). The exchange kinetics of DHE and radiolabeled cholesterol between model membranes was indistinguishable (117). For a kinetic sterol exchange assay between biological membranes, cellular organellar membranes can be isolated from cells supplemented with DHE to act as donors and without supplementation of DHE to act as acceptors. Not only exchange kinetics but also lifetime analysis resolved multiple sterol domains; and cholesterol binding/transfer proteins such as SCP-2 (and less so L-FABP) rapidly facilitated DHE transfer from these purified membrane fractions to other intracellular membranes *in vitro* (54,55). With regards to cholesterol movement between purified intracellular organelle membrane fractions, the most rapid spontaneous DHE transfer occurred from mitochondrial membranes to microsomal membranes, mitochondrial to lysosomal and to plasma membranes, and plasma membranes to microsomal membranes (173). Least rapid spontaneous DHE transfer occurred from lysosomal to plasma membranes. However, in the presence of the SCP-2, the DHE transfer was markedly enhanced in the approximate order of plasma membrane to microsomal membranes and plasma membranes to lysosomal membranes (173). This order was followed by enhanced transfer from mitochondrial membranes to microsomal membrane, mitochondrial membranes to plasma membranes, and a nearly equal transfer between mitochondrial and plasma membranes. Other than the transfer between mitochondrial and plasma membranes, the reverse transfer was

markedly slower in both spontaneous and SCP-2 mediated (173). Thus, *in vitro* exchange dynamics of DHE revealed that: (i) spontaneous sterol transfer was very slow, but vectorial; (ii) spontaneous sterol transfer from lysosomes and lysosomal membranes was extremely slow, despite the fact that this is the route of LDL-receptor mediated cholesterol uptake; (iii) cholesterol-binding proteins such as SCP-2 rapidly enhanced the extent and directional transfer of sterol transfer from lysosomes and lysosomal membranes to the plasma membrane.

### 6.5. Physiological Significance of *in vitro* Studies with DHE and other Fluorescent Sterols: Cultured Cells and Animals

The significance of the above findings in living cells was confirmed with DHE and other fluorescent sterols in a variety of cultured cells including L-cells, CHO cells, macrophages, and hepatocyte derived cell lines (39,43,45,160,174–176). Studies with transfected L-cells showed that uptake and efflux of fluorescent sterols was highly dependent on the expression of cholesterol binding proteins (*e.g.* such as SCP-2) in the cytosol. Furthermore, transhepatocyte transfer of DHE was very rapid and not vesicular. Since hepatocytes have very high levels of intracellular cholesterol binding proteins (*e.g.* SCP-2, L-FABP) taken together such data suggested that rapid transhepatocyte cholesterol trafficking from the basolateral to canalicular membrane for efflux was facilitated by these proteins in the cytosol. The physiological impact of cholesterol binding proteins such as SCP-2 and L-FABP on cholesterol uptake, esterification, and excretion into bile was confirmed by studies with SCP-2 transgenic (*i.e.* overexpressing or antisense cDNA treated) mice and rats (177–179) and gene-targeted mice wherein SCP-2/SCP-x (180–182), SCP-x (183), or L-FABP (184–189) were ablated.

Studies with radiolabeled cholesterol were consistent with many of the findings shown with the fluorescent DHE and other sterols in cultured cells (43,45,172,190–197). In one study, it was shown that overexpression of L-FABP in L-cell fibroblasts enhanced the transfer or radiolabled cholesterol from the plasma membrane to the endoplasmic reticulum for esterification (194). Transfer was inhibited by drugs that bound/competed with cholesterol for the L-FABP binding site. In another study L-cells were transfected with the cDNA that encodes for the 13.2 kDa and 15 kDa SCP-2 proteins respectively. In nearly all tissues and cells examined the 15 kDa SCP-2 undergoes complete N-terminal post-translational cleavage to yield the mature 13.2 kDa SCP-2 (rev. in (173). Despite the fact that only the 13.2 kDa protein was found in both cases, different effects on the intracellular trafficking of cholesterol were observed (191). In early experiments using radiolabeled cholesterol, 15 kDa SCP-2 transfected L-cells showed an enhanced uptake of [$^3$H]cholesterol after 4 hours including a resultant increase in esterification of the exogenous radiolabeled cholesterol as shown by the 30% increase in [$^3$H]cholesteryl ester levels with no enhancement in the 13.2 kDa SCP-2 transfected L-cells as compared to the control cells. Both the 15 kDa and the 13.2 kDa SCP-2 transfected L-cells showed a significant increase (15 and 11-fold, respectively) in the initial [$^3$H] cholesteryl ester synthesis rate compared to control cells after treatment with sphingomyelinase. This experiment was important in order to examine the effect of SCP-2 expression on the intracellular movement of cholesterol from the plasma membrane to the endoplasmic reticulum for esterification (192). The resulting data corresponded with the aforementioned fluorescent *in vitro* assays where greater enhancement occurred in the direction of exchange of DHE from plasma membrane to microsomal vesicle (6,173). The increased rate in ester synthesis resulted in a 1.5 increase in the [$^3$H]cholesteryl ester levels, while at saturation (1 hr treatment), the radiolabeled cholesteryl ester levels were increased 1.6 and 1.3 fold for 15 kDa and 13.2 kDa SCP-2 overexpression (192). Inhibition of microsomal cholesteryl ester synthesis by drug treatment in the sphingomyelinase treated cells showed no differences. The overexpression of 13.2 kDa SCP-2 did not elevate cholesterol homeostasis of free cholesterol while elevating esterified cholesterol levels (192). Treatment with [$^3$H]oleic acid revealed that the 15 kDa SCP-2 overexpression resulted in a specific increase of cholesterol esterification

as opposed to the 13.2 kDa SCP-2 overexpression which resulted in esterification into triacylglycerols(192). Using [$^3$H]cholesterol and the fluorescent 22-NBD-cholesterol in conjunction with high density lipoproteins (HDL), L-cells overexpressing SCP-2 were shown to inhibit the HDL mediated efflux of cholesterol of 61% and 157%, respectively (43). However, most of the inhibition occurred in the slower component while the faster component of the efflux pool (protein-mediated) was somewhat less affected. Clearly, both the radiolabeled cholesterol uptake and HDL-mediated 22-NBD-cholesterol efflux studies in living cells reveal that the effects of SCP-2 expression on cellular cholesterol transport become increasingly significant over longer time periods.

Overexpression of SCP-2 also had an inhibitory effect on the *in vitro* enhancement of SCP-2 on the exchange of DHE and cholesterol between purified lysosomal membranes as seen by the initial rates (8). Lipid analysis of lysosomal membranes revealed a significant decrease in the cholesterol to phospholipid ratio as a result of a small decrease in the cholesterol mass with a corresponding increase in phosphatidylserine; however, lyso-bis-phosphatidic acid (LBPA), which is involved in lysosomal cholesterol trafficking, was dramatically decreased by nearly 3-fold. Furthermore, sterol exchanges involving lysosomal membranes isolated from normal CWN human fibroblasts and NPC1 human fibroblasts revealed an apparent similar effect (25). The exchange of sterol from the fast kinetic pool was increased dramatically (2-fold increase in initial rate) upon addition of SCP-2 *in vitro* for the NPC1 lysosomal membranes when compared to the control CWN lysosomal membranes as determined by DHE polarization exchange assays. The decreased expression of SCP-2 in NPC1 fibroblasts, as seen in murine models of Niemann-Pick type C disease(198), allowed for a higher exchange rate of the fast kinetic pool as compared to CWN fibroblasts with larger normal expression of SCP-2. In fact, the lysosomal membranes from CWN human fibroblasts showed much slower spontaneous initial rate of sterol exchange as well. However, the trend was reversed in the slower but larger kinetic pool, where higher levels of SCP-2 caused a higher rate of sterol transfer *in vitro.* Both cell types exhibited similar sterol kinetic pool fractions for the isolated lysosomal membranes (25) despite differences in sterol transfer rates. With the exception of the pool fraction sizes, sterol transfer characteristics examined as a function of expression of SCP-2 in lysosomal membranes isolated from control and transfected murine fibroblasts appeared consistent with those seen in CWN and NPC1 human fibroblasts (8) possibly through membrane lipid domain alteration and/or involvement with LBPA (199). Exchanges between lysosomal donors to mitochondrial acceptors revealed similar results whereas SCP-2 overexpression removed the fast kinetic pool but enhanced the slower kinetic pool both in rate and in pool size (173). In the reverse exchange (mitochondrial donor to lysosomal acceptors), no fast kinetic pool was detected in the control. However, SCP-2 overexpression still reduced the early exchange of sterol as seen by the 6-fold reduction in initial rate by shifting most of the sterol into the non-exchangeable pool (173). In part, this might explain the large pool of non-exchangeable sterol observed in exchange assays using mitochondrial membrane vesicles isolated from steroidogenic MA-10 Leydig cells (143).

Thus, modulation of directional cholesterol transport and cholesterol esterification as well as membrane lipid composition has been demonstrated to occur as a function of expression levels of L-FABP or SCP-2, possibly through the interaction of proteins/receptors involved with cholesterol trafficking and lipid sensing/signaling. The resulting evidence has been obtained with assays using different labeled sterols including the fluorescent cholesterol analog DHE.

## 7. Plasma Membrane Sterol-rich Microdomains: *in vitro* studies

Based on findings with delivery of dansyl-cholesterol, the method and duration of fluorescent sterol delivery (e.g. micro-crystals, lipoproteins, LUV, or cyclodextrin complexes) may affect the distribution of fluorescent sterol to lipid rafts/caveolae or non-rafts (see Section 6.3 and

ref. (32). When transformed cells (L-cells, MDCK cells) or primary mouse hepatocytes were cultured with DHE (micro-crystals or LUV) under conditions to maximize DHE incorporation and equilibration, biochemical fractionation by affinity chromatography of purified plasma membrane vesicles yielded sterol-rich lipid rafts/caveolae, caveolae, and lipid rafts, respectively (26,27,70,136). DHE was codistributed similarly as cholesterol into sterol-rich and –poor domains (26,27,70,82,102,135,136,172,182,196). Lipid raft/caveolae associated receptors such as the oxytocin receptor are sensitive to the structure of the sterol with which it interacts and both cholesterol and DHE, but not other sterols, are effective in reconstituting activity of this highly sterol-sensitive plasma membrane protein in cholesterol-depleted lipid rafts/caveolae (89–91). DHE mobility (fluorescence polarization) differed significantly in lipid rafts/caveolae from non-rafts. While spontaneous DHE transfer from lipid rafts/caveolae was relatively slow, that from non-rafts was essentially non-detectable. SCP-2 dramatically enhanced DHE transfer from lipid rafts/caveolae, but not from non-raft domains. Further examination of the plasma membrane cholesterol partitioning revealed that sterol transfer, as resolved using DHE in fluorescence polarization kinetic assays, from caveolae/raft domains with introduction of SCP-2 was enhanced as compared to plasma membrane vesicles (136). Principally, the initial rate of the caveolae/raft fractions was increased by a factor of 5 with a larger portion of the sterol arranged in an exchangeable kinetic pool as compared to the overall plasma membrane fraction (136). A possible mechanism for this enhancement may involve: (i) SCP-2 directly binding cholesterol as shown by fluorescent sterol binding assays and cross-linking by photoactivatable cholesterol (Fig. 1B) (39–41,44); (ii) SCP-2 directly interacting with caveolin-1 within the plasma membrane as observed from *in vitro* (coIP, CD) and *in vivo* (two hybrid, double immunofluorescence FRET, double immunogold EM) assays that revealed an average molecular interaction distance of ~48Å was measured (200). Specifically, SCP-2 has been shown to directly interact with the N-terminal sequence of amino acids of caveolin-1 (201). Finally, DHE transfer from lipid rafts/caveolae to serum lipoproteins was remarkably specific for the type of lipoprotein/apoprotein, while that to non-rafts was very slow and not specific (27). The importance of resolving cholesterol structure and dynamics in these cholesterol-rich plasma membrane microdomains is underscored by the fact that lipid rafts/caveolae function not only in reverse cholesterol transport, but also in cell recognition, signaling, immune function, and potocytosis (rev. in (58,60,82,84,85,87). Furthermore, lipid rafts/caveolae were shown to mediate the action of potential bioterror toxins and serve as entry portals for a host of bioterror pathogens (rev. in (82,202).

## 8. Plasma Membrane Sterol-rich Microdomains: real-time imaging of DHE in plasma membranes of living cells

Recent improvements in imaging microscopy allowed the direct, real-time visualization of DHE in living cells by conventional (DHE delivered as micro-crystals) or video (DHE delivered as cyclodextrin complexes) UV fluorescence microscopy (39,160,174–176) and by MPLSM (DHE delivered as LUV or micro-crystals) multiphoton laser scanning microscopy (71,82,203,204). Analysis of intracellular localization and distribution of DHE at the plasma membrane can be accomplished after segmentation of specific regions of interest such as cellular organelles and performed on a cell by cell basis (70,203). Previously, two techniques involving image segmentation of the plasma membrane of cells labeled with DHE and multiple fluorescent probes (*i.e.* Nile Red, ECFP-Mem, and DiO) were validated and compared (203): (i) subtraction and sliding window and (ii). rank statistic-based methodology. The subtraction technique was performed with the DHE and Nile Red colocalization experimental results by subtracting the DHE channel from the Nile Red channel. This procedure worked very well with Nile Red as it only very weakly stained the PM as compared to the significantly brighter labeling by the DHE. Noise was reduced by using a sliding window analysis technique where window size, intensity thresholding, and the signal to noise ratio was optimized. In the rank

stastic-based technique, two small windows are created in the image and the pixel intensities in each window ranked from the lowest to highest; then a comparison is made by using Miller's rank statistic. The solution is optimized based upon intensity thresholding. The segmented plasma membrane regions were smoothed using geometric moments functions based on the intensity distribution within the segmented PM. Subsequently, geometric reference and spatial intensity measurements were calculated. Spatial statistical analysis was performed using pixels with DHE intensities higher than the median intensity to test for complete spatial randomness (CSR). Monte Carlo simulations were run using the narrowed data set (peak intensities—relative higher concentrations) as well as the complete data set (203).

### 8.1. Multiphoton imaging of DHE incorporated into L-cells from ethanolic stock diluted in aqueous medium

L-cell fibroblasts grown on chambered coverglass were incubated with the fluorescent sterol analog, DHE, from ethanolic stock solution as described above and imaged by multi-photon microscopy. Despite multiple washings of the cells, images from a single channel covering the range 350–450 nm revealed very bright patches of fluorescence emission (Fig. 6A). By monitoring the ratio of the 455 nm region to 375 nm region, the areas that were either mostly micro-crystalline or mostly monomeric were distinguished (70). The micro-crystalline DHE phagocytosed by the cells was largely found to be in lysosomes (70) but breakdown of the microcrystals occured over time (~2-3 days) such that monomeric DHE was distributed throughout the cell into the plasma membrane, lipid storage droplets, endoplasmic reticulum, and other organellar membranes. This was also observed in organelles isolated from cells incubated for several days on DHE from ethanolic stock solution (6,8,70,102,129). As a result of the increased localized concentration of micro-crystalline DHE and its enhanced excimeric fluorescence, difficulties arise in detecting low to moderate amounts of monomeric DHE (Fig. 6A:inset). This is due to the intense emission arising from crystalline DHE which can cause saturation of the PMTs (70,204). Plasma membrane sterol can be detected by imaging cells that do not have residual large amounts of crystalline DHE.

### 8.2. Multiphoton imaging of DHE incorporated into L-cells from LUV diluted in medium

DHE in the form of LUVs was taken up by living cells (Fig. 6B) in largely monomeric form as indicated by the emission peak ratios (70). There was almost no appearance of DHE micro-crystals (70). As a result, sensitivity of detection can be increased by using an emission dichroic/filter combination with broader bandwidth and higher photomultiplier gain. Thus, DHE with its low quantum yield can easily be detected at the plasma membrane (Fig. 6B: inset) and in intracellular compartments as had been observed from previous spectroscopic studies(8,70, 102,135,172). Signal saturation may occur as a result of accumulation of unesterified or esterified monomeric DHE in lipid storage vesicles (Fig. 6B), distinct and much less intense than microcrystalline DHE observed in lysosomes upon culturing cells with DHE micro-crystals. MPLSM images of cells supplement with DHE as LUV revealed that DHE was non-randomly distributed into sterol-rich and poor- domains within the plasma membrane of living L-cells (70,203,204).

### 8.3. Multiphoton imaging of DHE incorporated into L-cells from DHE-MβCD complexes diluted in aqueous medium

L-cell incubation with DHE-MβCD complexes also yielded the monomeric DHE form as visualized by real-time multi-photon imaging in a confocal slice through the cell (Fig. 6). Within 45 minutes, heterogeneous regions of the plasma membrane were strongly labeled with DHE (Fig. 6C:inset), evidenced by the strong patchy outline at the cellular periphery. Other intracellular membranes were weakly labeled throughout the cell (Fig. 6C). In many of the cells, morphological structures such as microvilli and filopodia were also visible as a result of

the strong signal from the fluorescent DHE. The non-random distribution of DHE in to sterol-rich and poor- domains at the plasma membrane was consistent with other studies wherein DHE was supplemented as LUV to the cells (70,203,204). This would suggest that supplementation of cells with DHE-MβCD complexes also non-selectively loaded the different domains in the plasma membrane.

### 8.4. Image analysis of DHE distribution after multiphoton imaging

While MPLSM and visual inspection of DHE at the plasma membrane of cells supplemented with DHE as micro-crystals, LUV, or DHE-MβCD complexes revealed that DHE was non-randomly distributed into sterol-rich and poor- domains, a mathematical framework substantiating this observation requires additional analysis (70,203,204).

Image analysis originally consisted of intensity measurements using region of interests and the use of colocalization, ratiometric, and fluorogram techniques. Further structured segmentation of the plasma membrane has permitted examination of the distribution of DHE through the use of inferential statistics, utilizing hypothesis testing and correlation determination, and has opened up an opportunity to do distributional modeling (71,203). Segmenation analysis of the MPLSM images of cells supplement with DHE as LUV confirmed that DHE was indeed non-randomly distributed into sterol-rich and poor- domains within the plasma membrane of living L-cells (203,204).

## 9. Summary and Discussion

The naturally-occurring fluorescent sterol DHE (19,21) has proven a powerful probe for use in investigating membrane structure and cholesterol domain dynamics *in vitro* (8,54,55,65, 70,102,172), for examining cholesterol-protein interactions *in vitro* (2,39,96,101,102,108, 205), and for first time visualization in real-time of the distribution of cholesterol in the plasma membranes in living cells (70,203,204). Successful application of the fluorescent DHE to investigation of the function and organization of sterols in membranes, especially lipid raft/caveolae microdomains of living cells, requires the use of highly purified DHE. This is due to the fact that lipid rafts/caveolae are highly sensitive not only to cholesterol content (58,60, 82,84,85,87,88), but also to sterol structure (89), and sterol oxidation. The present review yielded new insights into this problem and potential applications of DHE imaging in living cells.

The presence of a non-fluorescent sterol impurity was observed not only in commercially available DHE, but also in DHE synthesized in the present laboratory from ergosterol obtained from multiple commercial sources. The appearance of the non-fluorescent sterol impurity was somewhat variable (20–40%) depending on the commercial source and batch of the ergosterol substrate but without dependence on any other reagent used for the synthesis. While both HPLC and APCI mass spectroscopy suggested that the impurity was either ergosterol or an ergosterol isomer, the unique UV spectral absorption characteristics of this impurity provided evidence that the non-fluorescent sterol impurity was an isomer of the initial ergosterol (5,7,22-cholestatrien-24β-methyl-3β-ol). This isomer, known as ergosterol D [*i.e.*, 7,9(11),22-cholestatrien-24β-methyl-3β-ol], was not present in the ergosterol starting material but potentially arose from the rearrangement of double bonds in the B ring of the ergosterol during the dehydration step (Step IIA, Fig. 5). Purifying the ergosterol created a non-detectable yield of the ergosterol D impurity during DHE synthesis. While the nature of the water soluble component facilitating formation of the side reaction ergosterol D isomer was not identified, it has been reported that small amounts of nitric acid or mercuric nitrate catalyze the formation of the tetraene DHE as well as a side product, *i.e.*, mercurated triene, and so such impurities may be possible contaminants in the original ergosterol (64).

Recently, real-time multiphoton imaging of the naturally-occurring fluorescent sterol DHE in the plasma membrane of living cells (70,82,203,204) was used to examine sterol distribution directly with high optical sectioning capability (206–209). While subcellular distribution (plasma membrane, lysosome, lipid droplet, etc) of DHE was highly dependent on the method of delivery (microcrystals, LUV, MβCD), DHE at the plasma membrane was found to be distributed non-randomly into sterol-rich and sterol-poor regions in plasma membranes of living cells with the size range of sterol-rich clustering domains estimated to be from 200 nm (limit of optical microscopy) to 565 nm (70,71,82,203). Due to the diffraction limit of resolution, there is uncertainty about whether these regions, as visible under laser scanning microscopy, are contiguous lateral domains (70,71,203) or represent artificial enhancement of the intensity as a result of microvillar/filipodia extensions and/or folding (210,211) of the plasma membrane.

Video imaging studies involving HepG2 cells had resolved regions in the size range of 2000–3000 nm and had shown evidence of sterol-rich and sterol-poor distribution in the plasma membrane as well as canalicular microvilli of the polarized cells (210). It was concluded, however, that these were not regions of enrichment but represented microvilli (210). This same conclusion was reached following subsequent video imaging studies involving methyl-β-cyclodextrin complexes using a pulse chase method and the cell lines Hep G2, J774, and TRVb1 (211) where artifactual enhancement of the fluorescent emission was the result of rough surface topology and cell protrusions (211). However, other studies using filipin, which labels all cholesterol in the plasma membrane without differentiating between sterol-rich or sterol-poor, did not reveal any enhancement in intensity as a result of plasma membrane ruffling or tubule sizing issues (212,213).

Differences in results obtained by video imaging may be due to several factors: strong photobleaching of the fluorescent sterol as a result of video imaging techniques, saturation of all the plasma membrane with fluorescent sterol for video imaging, and video imaging's weak resolution in the Z-axis facilitating the need for deconvolution. In contrast, the MPLSM imaging studies used a loading methodology wherein only small amounts (non-saturable) of DHE were introduced into the plasma membrane over longer period of time to minimize the initial perturbations within the membrane (70,71,203). With multi-photon excitation used in MPLSM, less extraneous photobleaching of the fluorescent sterol occurred with fluorescence emission from only the excitation volume at a radial resolution on the order of 300 nm while shorter dwell times minimized photodamage. The combination of probing sterol organization and distribution with low amounts of fluorescent sterol together with the resolution enhancement resulting from low yield in the 3-photon excitation volume element, cross-interference from the rough surface topology was reduced.

Available data from many experimental studies of the plasma membrane in general suggest cholesterol is the driving force for microdomain formation and cholesterol is not uniformly or homogeneously distributed but that the plasma membrane of living cells consists of areas of cholesterol segregation (regions that are cholesterol-rich and cholesterol-poor) (56,214). Biochemical studies also support this concept and demonstrate that purified cholesterol-rich microdomains isolated from cultured cell (L-cell, MDCK, primary hepatocytes) represent nearly one-third of the plasma membrane, are rich in cholesterol as well as saturated/monounsaturated fatty acylated phospholipids, and are comprised of physically distinct, liquid-ordered membrane phases intermediate between fluid liquid-crystalline and rigid gel phases (26,82,102,136,172,182,215–217). Studies with purified microdomains from L-cell and MDCK plasma membranes showed that both exogenous (*e.g.* HDL) and endogenous (*e.g.* SCP-2) cholesterol binding proteins preferentially donate or extract cholesterol from cholesterol-rich, but not cholesterol-poor, microdomains (26,27,136,137,172). The microdomain/lipid raft concept, despite controversy in details, provides a framework for

biologists studying localization and function of membrane protein receptors, transporters, and downstream signaling molecules that regulate uptake of cholesterol (86,87,218–239), fatty acids (240–242), glucose (243–254), and other activities (216,255–260).

## Acknowledgements

This work was supported in part by the by the USPHS, NIH GM31651 (FS, ABK), GM72041 (Project 2, ABK,FS), and Mentored Quantitative Research Career Development Award (K25) DK062812 (AMG).

## Abbreviations

**DHE**
dehydroergosterol

**DHE-MβCD**
DHE-methyl-β-cyclodextrin

**SP**
spin-labeled

**BODIPY**
4,4-difluoro-4-bora-3a,4a-diaza-*s*-indacene

**NBD**
*N*-(7-nitrobenz-2-oxa-1,3-diazol-4-yl)amino

**Dansyl**
5-dimethylaminonapthalene-1-sulfonyl

**CTE**
cholestatrienol

**DiO**
3,3'-dioctadecyloxacarbocyanine perchlorate

**ECFP**
enhanced cyan fluorescent protein

**BHT**
butylatedhydroxytoluene

**APCI**
(atmospheric pressure chemical ionization) mass spectroscopy

**HPLC**
high performance liquid chromatography

**LUV**
large unilamellar vesicle

**SCP-2**
sterol carrier protein-2

**L-FABP**
liver fatty acid binding protein

**MDCK**
Madin-Darby canine kidney

**EPR**

electron spin resonance

## Reference List


1. Haberland ME, Reynolds JA. Self-association of cholesterol in aqueous solution. Proc Natl Acad Sci 1973;70:2313–2318. [PubMed: 4525165]
2. Fischer RT, Cowlen MS, Dempsey ME, Schroeder F. Fluorescence of delta 5,7,9(11),22-ergostatetraen-3 beta-ol in micelles, sterol carrier protein complexes, and plasma membranes. Biochemistry 1985;24:3322–3331. [PubMed: 4027244]
3. Fischer RT, Stephenson FA, Shafiee A, Schroeder F. delta 5,7,9(11)-Cholestatrien-3 beta-ol: a fluorescent cholesterol analogue. Chem Phys Lipids 1984;36:1–14. [PubMed: 6518610]
4. Avdulov NA, Chochina SV, Igbavboa U, Warden CH, Schroeder F, Wood WG. Lipid binding to sterol carrier protein-2 is inhibited by ethanol. Biochim Biophys Acta 1999;1437:37–45. [PubMed: 9931423]
5. Castanho MA, Brown W, Prieto M. Rod-like cholesterol micelles in aqueous solution studied using polarized and depolarized dynamic light scattering. Biophys J 1992;63:1455–1461. [PubMed: 1489905]
6. Frolov A, Woodford JK, Murphy EJ, Billheimer JT, Schroeder F. Spontaneous and protein-mediated sterol transfer between intracellular membranes. J Biol Chem 1996;271:16075–16083. [PubMed: 8663152]
7. Frolov AA, Woodford JK, Murphy EJ, Billheimer JT, Schroeder F. Fibroblast membrane sterol kinetic domains: modulation by sterol carrier protein 2 and liver fatty acid binding protein. J Lipid Res 1996;37:1862–1874. [PubMed: 8895052]
8. Gallegos AM, Atshaves BP, Storey SM, Schoer J, Kier AB, Schroeder F. Molecular and fluorescent sterol approaches to probing lysosomal membrane lipid dynamics. Chem Phys Lipids 2002;116:19–38. [PubMed: 12093533]
9. Holthuis JCM, Levine TP. Lipid traffic: floppy drives and superhighway. Nature Rev Mol Cell Biol 2005;6:209–220. [PubMed: 15738987]
10. Warren, RC. Membrane microscopy. In: Warren, RC., editor. Physics and the architecture of cell membranes. Adam Hilger; Bristol, England: 1987. p. 48-69.
11. Warren, RC. Membrane crystallography. In: Warren, RC., editor. Physics and the architecture of cell membranes. Adam Hilger; Bristol, England: 1987. p. 70-108.
12. Schroeder, F.; Nemecz, G. Transmembrane Cholesterol Distribution. In: Esfahami, M.; Swaney, J., editors. Advances in Cholesterol Research. Telford Press; Caldwell, NJ: 1990. p. 47-87.
13. Small, DM. The Physical Chemistry of Lipids. Plenum Press; New York: 1986. p. 276
14. Warren, RC. Thermal analysis. In: Warren, RC., editor. Physics and the architecture of cell membranes. Adam Hilger; Bristol, England: 1987. p. 109-121.
15. Warren, RC. Membrane magnetic resonance. In: Warren, RC., editor. Physics and the architecture of membranes. Adam Hilger; Bristol, England: 1987. p. 122-162.
16. Scheidt HA, Muller P, Herrmann A, Huster D. The potential of fluorescent and spin-labeled steroid analogues to mimic natural cholesterol. J Biol Chem 2003;278:45563–45569. [PubMed: 12947110]
17. Badley, RA. Fluorescent probing of dynamic and molecular organization of biological membranes. In: Wehry, EL., editor. Modern Fluorescence Spectroscopy. 2. Plenum Press; New York, NY: 1976. p. 91-168.
18. Wechsler A, Brafman A, Shafir M, Heverin M, Gottlieb H, Damari G, Gozlan-Kelner S, Spivak I, Moshkin O, Fridman E, Becker Y, Skaliter R, Einat P, Faerman A, Bjorkhem I, Feinstein E. Generation of viable cholesterol-free mice. Science 2003;302:2087. [PubMed: 14684813]
19. Sica D, Boniforti L, DiGiacomo G. Sterols of candida tropicalis grown on n-alkanes. Phytochemistry 1982;21:234–236.
20. Bocking T, Barrow KD, Netting AG, Chilcott TC, Coster HGL, Hofer M. Effects of singlet oxygen on membrane sterols in the yeast Saccaromyces cerevisiae. FEBS Lett 2000;267:1607–1618.

21. Delseth C, Kashman Y, Djerassi C. Ergosta-5,7,9(11),22-tetraen-3beta-ol and its 24epsilon-ethyl homolog, two new marine sterols from the red sea sponge Biemna fortis. Helv Chim Acta 1979;62:2037–2045.
22. Rothblat GH, Burns CH, Conner RL, Landrey JR. Desmosterol as the major sterol in L-cell mouse fibroblasts grown in sterol free culture medium. Science 1970;169:880–882. [PubMed: 5432584]
23. Schroeder F, Perlmutter JF, Glaser M, Vagelos PR. Isolation and characterization of mammalian membranes with altered phospholipid composition from cultured fibroblasts. J Biol Chem 1976;251:6739–6746. [PubMed: 977594]
24. Hale JE, Schroeder F. Asymmetric transbilayer distribution of sterol across plasma membranes determined by fluorescence quenching of dehydroergosterol. Eur J Biochem 1982;122:649–661. [PubMed: 7060596]
25. Schroeder F, Gallegos AM, Atshaves BP, Storey SM, McIntosh A, Petrescu AD, Huang H, Starodub O, Chao H, Yang H, Frolov A, Kier AB. Recent advances in membrane cholesterol microdomains: rafts, caveolae, and intracellular cholesterol trafficking. Experimental Biology and Medicine 2001;226:873–890. [PubMed: 11682693]
26. Gallegos AM, Storey SM, Kier AB, Schroeder F, Ball JM. Stucture and cholesterol dynamics of caveolae/raft and nonraft plasma membrane domains. Biochem 2006;45:12100–12116. [PubMed: 17002310]
27. Storey SM, Gallegos AM, Atshaves BP, McIntosh AL, Martin GG, Landrock K, Kier AB, Ball JA, Schroeder F. Selective cholesterol dynamics between lipoproteins and caveolae/lipid rafts. Biochem 2007;46:13891–13906. [PubMed: 17990854]
28. Fliesler SJ, Richards MJ, Miller CY, Cenedella RJ. Cholesterol synthesis in the vertebrate retina: effects of U1866A on rat retinal struture, photoreceptor membrane assembly, and sterol metabolism and composition. Lipids 2000;35:289–296. [PubMed: 10783006]
29. Heverin M, Meaney S, Brafman A, Shafir M, Olin M, Shafaati M, von Bahr S, Larsson L, Lovgren-Sandblom A, Diczfalusy U, Parini P, Feinstein E, Bjorkhem I. Studies on the cholesterol-free mouse: Strong activation of LXR-regulted hepatic genes when replacing cholesterol with desmosterol. Arterioscler Thromb Vasc Biol 2007;27:2191–2197. [PubMed: 17761942]
30. Wang P, Spencer TA. Preparation of isotopicallly labelled benzophenone-containing lipid analogues. J Labelled Compd Radiopharm 2005;48:781–788.
31. Wiegand V, Chang TY, Strauss JF III, Fahrenholz F, Gimpl G. Transport of plasma membrane derived cholesterol and the function of Niemann-Pick C1 protein. FASEB J 2003;17:782–784. [PubMed: 12594172]
32. Huang H, McIntosh AL, Atshaves BP, Kier AB, Schroeder F. Polarity sensitive dansyl-cholesterol as a probe for sterol-rich and -poor domains in plasma membranes of living cells. Biochemistry Submitted. 2008
33. Li Z, Mintzer E, Bittman R. First synthesis of free cholesterol-BODIPY conjugates. J Org Chem 2005;71:1718–1721. [PubMed: 16468832]
34. Li Z, Bittman R. Synthesis and spectral properties of cholesterol- and FTY720-containing boron dipyrromethene dyes. J Org Chem 2007;72:8367–8382.
35. Chattopadhyay A, London E. Parallax method for direct measurement of membrane penetration depth utilizing fluorescence quenching by spin-labeled phospholipids. Biochem 1987;26:39–45. [PubMed: 3030403]
36. Mukherjee S, Chattopadhyay A. Membrane organization at low cholesterol concentrations: A study using NBD- labeled cholesterol. Biochemistry 1996;35:1311–1322. [PubMed: 8573588]
37. Mukherjee S, Chattopadhyay A. Monitoring cholesterol organization in membranes at low concentrations utilizing the wavelength-selective fluorescence approach. Chem Phys Lip 2005;134:79–84.
38. Shaw JE, Epand RF, Epand RM, Li Z, Bittman R, Yip CM. Correlated fluorescence-atomic force microscopy of membrane domains: Structure of fluorescence probes determines lipid localization. Biophys J 2006;90:2170–2178. [PubMed: 16361347]
39. Schroeder, F.; Frolov, A.; Schoer, J.; Gallegos, A.; Atshaves, BP.; Stolowich, NJ.; Scott, AI.; Kier, AB. Intracellular sterol binding proteins, cholesterol transport and membrane domains. In: Chang,

TY.; Freeman, DA., editors. Intracellular Cholesterol Trafficking. Kluwer Academic Publishers; Boston: 1998. p. 213-234.

40. Stolowich NJ, Frolov A, Petrescu AD, Scott AI, Billheimer JT, Schroeder F. Holo-sterol carrier protein-2: $^{13}$C-NMR investigation of cholesterol and fatty acid binding sites. J Biol Chem 1999;274:35425–35433. [PubMed: 10585412]
41. Schroeder F, Frolov A, Starodub O, Russell W, Atshaves BP, Petrescu AD, Huang H, Gallegos A, McIntosh A, Tahotna D, Russell D, Billheimer JT, Baum CL, Kier AB. Pro-sterol carrier protein-2: role of the N-terminal presequence in structure, function, and peroxisomal targeting. J Biol Chem 2000;275:25547–25555. [PubMed: 10833510]
42. Serrero G, Frolov A, Schroeder F, Tanaka K, Gelhaar L. Adipose differentiation related protein. Expression, purification of recombinant protein in E. coli and characterization of its fatty acid binding properties. Biochim Biophys Acta 2000;1488:245–254. [PubMed: 11082534]
43. Atshaves BP, Starodub O, McIntosh AL, Roths JB, Kier AB, Schroeder F. Sterol carrier protein-2 alters HDL-mediated cholesterol efflux. J Biol Chem 2000;275:36852–36861. [PubMed: 10954705]
44. Martin GG, Hostetler HA, Tichy SE, Russell DH, Berg JM, Woldegiorgis G, Spencer TA, Ball JA, Kier AB, Schroeder F. Structure and function of the sterol carrier protein-2 (SCP-2) N-terminal pre-sequence. Biochemistry 2008;47:5915–5934. [PubMed: 18465878]
45. Frolov A, Petrescu A, Atshaves BP, So PTC, Gratton E, Serrero G, Schroeder F. High density lipoprotein mediated cholesterol uptake and targeting to lipid droplets in intact L-cell fibroblasts. J Biol Chem 2000;275:12769–12780. [PubMed: 10777574]
46. Portioli Silva EP, Peres CM, Mendonca JR, Curi R. NBD-cholesterol incorporation by rat macrophages and lymphocytes: a process dependent on the activation state of the cells. Cell Biochem and Function 2004;22:23–28.
47. Schroeder F, Zhou M, Swaggerty CL, Atshaves BP, Petrescu AD, Storey S, Martin GG, Huang H, Helmkamp GM, Ball JM. Sterol carrier protein-2 functions in phosphatidylinositol transfer and signaling. Biochemistry 2003;42:3189–3202. [PubMed: 12641450]
48. Gadella TW, Wirtz KW. Phospholipid binding and transfer by non-specific lipid transfer protein (SCP-2): a kinetic model. Eur J Biochem 1994;220:1019–1028. [PubMed: 8143718]
49. Frolov A, Cho TH, Billheimer JT, Schroeder F. Sterol carrier protein-2, a new fatty acyl coenzyme A-binding protein. J Biol Chem 1996;271:31878–31884. [PubMed: 8943231]
50. Dansen TB, Westerman J, Wouters F, Wanders RJ, van Hoek A, Gadella TW, Wirtz KW. High affinity binding of very long chain fatty acyl CoA esters to the peroxisomal non-specific lipid transfer protein (sterol carrier protein-2). Biochem J 1999;339:193–199. [PubMed: 10085244]
51. Pfanner N, Glick BS, Arden SR, Rothman JE. Fatty acylation promotes fusion of transport vesicles with Golgi cisternae. J Cell Biol 1990;110:955–961. [PubMed: 2324202]
52. Pfanner N, Orci L, Glick BS, Amherdt M, Arden SR, Malhotra V, Rothman JE. Fatty acyl CoA is required for budding of transport vesicles from Golgi cisternae. Cell 1989;59:95–102. [PubMed: 2790961]
53. Schroeder F, Atshaves BP, McIntosh AL, Gallegos AM, Storey SM, Parr RD, Jefferson JR, Ball JM, Kier AB. Sterol carrier protein-2: New roles in regulating lipid rafts and signaling. Biochim Biophys Acta 2007;1771:700–718. [PubMed: 17543577]
54. Schroeder F, Jefferson JR, Kier AB, Knittell J, Scallen TJ, Wood WG, Hapala I. Membrane cholesterol dynamics: cholesterol domains and kinetic pools. Proc Soc Exp Biol Med 1991;196:235–252. [PubMed: 1998001]
55. Schroeder F, Frolov AA, Murphy EJ, Atshaves BP, Jefferson JR, Pu L, Wood WG, Foxworth WB, Kier AB. Recent advances in membrane cholesterol domain dynamics and intracellular cholesterol trafficking. Proc Soc Exp Biol Med 1996;213:150–177. [PubMed: 8931661]
56. Bretscher MS, Munro S. Cholesterol and the Golgi apparatus. Science 1993;261:1280–1281. [PubMed: 8362242]
57. Smart EJ, Ying Y, Mineo C, Anderson RGW. A detergent-free method for purifying caveolae membrane from tissue culture cells. Proc Natl Acad Sci 1995;92:10404–10408.
58. Brown DA, London E. Structure and function of sphingolipid- and cholesterol-rich membrane rafts. J Biol Chem 2000;275:17221–17224. [PubMed: 10770957]

59. Brown DA, London E. Structure and origin of ordered lipid domains in biological membranes. J Membr Biol 1998;164:103–114. [PubMed: 9662555]
60. Anderson RGW, Jacobson K. A role for lipid shells in targeting proteins to caveolae, rafts, and other lipid domains. Science 2002;296:1821–1825. [PubMed: 12052946]
61. Jacobson K, Vaz WL. Domains in biological membranes. Comments Mol Cell Biophys 1992;8:1–15.
62. Pike LJ. Lipid rafts: heterogeneity on the high seas. Biochem J 2004;378:281–292. [PubMed: 14662007]
63. Pike LJ. Rafts defined : A report on the Keystone symposium on lipid rafts and cell function. J Lipid Res 2006;47:1597–1598. [PubMed: 16645198]
64. Ruyle WV, Jacob TA, Chemerda JM, Chamberlin EM, Rosenburg DW, Sita GE, Erickson RL, Aliminosa LM, Tishler M. The preparation of delta7,9(11)-allo-steroids by the action of mercuric acetate on delta7-allo steroids. J Am Chem Soc 1953;75:2604–2609.
65. Schroeder F. Fluorescent sterols: probe molecules of membrane structure and function. [Review]. Prog Lipid Res 1984;23:97–113. [PubMed: 6387716]
66. Gimpl G, Gehrig-Burger K. Cholesterol reporter molecules. Bioscience Report. 200710.1007/s10540-007-9060-1
67. Wustner D. Fluorescent sterols as tools in membrane biophysics and cell biology. Chem Phys Lip 2007;146:1–25.
68. McIntosh, AL.; Huang, H.; Atshaves, BP.; Kier, AB.; Schroeder, F. Fluorescent sterols to study cholesterol trafficking in living cells. In: Miller, L., editor. Selective Probes and Tags to Study Biomolecular Function In Vivo. Wiley VCH; Weinheim: 2007. In press
69. Fischer RT, Stephenson FA, Shafiee A, Schroeder F. Structure and dynamic properties of dehydroergosterol, delta 5,7,9(11),22-ergostatetraen-3 beta-ol. J Biol Phys 1985;13:13–24.
70. McIntosh A, Gallegos A, Atshaves BP, Storey S, Kannoju D, Schroeder F. Fluorescence and multiphoton imaging resolve unique structural forms of sterol in membranes of living cells. J Biol Chem 2003;278:6384–6403. [PubMed: 12456684]
71. McIntosh, AL.; Atshaves, BP.; Huang, H.; Gallegos, AM.; Kier, AB.; Schroeder, F.; Xu, H.; Zhang, W.; Liu, S. Multiphoton laser scanning microscopy and spatial analysis of dehydroergosterol distributions on plasma membrane of living cells. In: McIntosh, TJ., editor. Lipid Rafts. 398. Humana Press; Totowa, NJ: 2007. in press
72. Bittman, R. A review of the kinetics of cholesterol movement between donor and acceptor bilayer membranes. In: Finegold, L., editor. Cholesterol in Membrane Models. CRC Press; Baton Raton, FL: 1993. p. 45-66.
73. Kan CC, Yan J, Bittman R. Rates of spontaneous exchange of synthetic radiolabeled sterols between lipid vesicles. Biochemistry 1992;31:1866–1874. [PubMed: 1737039]
74. Bittman R, Clejan S, Hui SW. Increased rates of lipid exchange between Mycoplasma capricolum membranes and vesicles in relation to the propensity of forming nonbilayer lipid structures. J Biol Chem 1990;265:15110–15117. [PubMed: 2394716]
75. Clejan S, Bittman R. Distribution and movement of sterols with different side chain structures between the two leaflets of the membrane bilayer of mycoplasma cells. J Biol Chem 1984;259:449–455. [PubMed: 6706946]
76. Abbott AJ, Nelsestuen GL. Association of a protein with membrane vesicles at the collisional limit: studies with blood coagulation factor Va light chain also suggest major differences between small and large unilamellar vesicles. Biochemistry 1987;26:7994–8003. [PubMed: 3427119]
77. McLean LR, Phillips M. Cholesterol transfer from small and large unilamellar vesicles. Biochim Biophys Acta 1984;776:21–26. [PubMed: 6477902]
78. Small DM. Progression and regression of atherosclerotic lesions. Insights from lipid physical chemistry. Arteriosclerosis 1988;8:103–129. [PubMed: 3348756]
79. Small DM, Shipley GG. Physical-chemical basis of lipid deposition in atherosclerosis. Science 1974;185:222–229. [PubMed: 4833824]
80. Tangirala RK, Jerome WG, Jones NL, Small DM, Johnson WJ, Glick JM, Mahlberg FH, Rothblat GH. Formation of cholesterol monohydrate crystals in macrophage-derived foam cells. J Lipid Res 1994;35:93–104. [PubMed: 8138726]

81. Smart EJ, Ying Y, Conrad PA, Anderson RGW. Caveolin moves from caveolae to the golgi apparatus in response to cholesterol oxidation. J Cell Biol 1994;127:1185–1197. [PubMed: 7962084]
82. Schroeder, F.; Atshaves, BP.; Gallegos, AM.; McIntosh, AL.; Liu, JC.; Kier, AB.; Huang, H.; Ball, JM. Lipid rafts and caveolae organization. In: Frank, PG.; Lisanti, MP., editors. Advances in Molecular and Cell Biology. 36. Elsevier; Amsterdam: 2005. p. 3-36.
83. Anderson R. The caveolae membrane system. Ann Rev Biochem 1998;67:199–225. [PubMed: 9759488]
84. Lavie Y, Liscovitch M. Changes in lipid and protein constituents of rafts and caveolae in multidrug resistant cancer cells and their functional consequences. Glycoconjugate Journal 2000;17:253–259. [PubMed: 11201798]
85. Everson WV, Smart EJ. Influence of caveolin, cholesterol, and lipoproteins on nitric oxide synthase. TCM 2001;11:246–250. [PubMed: 11673056]
86. Everson, WV.; Smart, EJ. Caveolae and the regulation of cellular cholesterol homeostasis. In: Lisanti, MP.; Frank, PG., editors. Caveolae and Lipid Rafts: Roles in Signal Transduction and the Pathogenesis of Human Disease. 36. Elsevier Academic Press; San Diego: 2005. p. 37-55.
87. Smart, EJ.; van der Westhuyzen, DR. Scavenger receptors, caveolae, caveolin, and cholesterol trafficking. In: Chang, TY.; Freeman, DA., editors. Intracellular Cholesterol Trafficking. Kluwer Academic Publishers; Boston: 1998. p. 253-272.
88. Kirsch C, Eckert GP, Mueller WE. Statins affect cholesterol micro-domains in brain plasma membranes. Biochem Pharmacol 2002;65:843–856. [PubMed: 12628479]
89. Burger K, Gimpl G, Fahrenholz F. Regulation of receptor function by cholesterol. Cell Mol Life Sci 2000;57:1577–1592. [PubMed: 11092453]
90. Gimpl G, Burger K, Fahrenholz F. Cholesterol as modulator of receptor function. Biochemistry 1997;36:10959–10974. [PubMed: 9283088]
91. Gimpl G, Fahrenholz F. Human oxytocin receptors in cholesterol-rich vs cholesterol-poor microdomains of the plasma membrane. Eur J Biochem 2000;267:2483–2497. [PubMed: 10785367]
92. Bergmann W, Klacsmann JA. Ergosterol F. J Org Chem 1947;13:21–25. [PubMed: 18917704]
93. Bergmann W, Stevens PG. Studies on the conversion of ergosterol to adrenal cortical hormones. J Org Chem 1947;13:10–25. [PubMed: 18917703]
94. Budziarek R, NewboldG T, Stevenson R, Spring FS. Steroids. Part I. 11-oxygenated steroids from ergosteryl-D acetate. J Chem Soc 1952 July;(Part 3):2892–2900.
95. Smutzer G, Crawford BF, Yeagle PL. Physical properties of the fluorescent sterol probe dehydroergosterol. Biochim Biophys Acta 1986;862:361–371. [PubMed: 3778897]
96. Loura LMS, Prieto M. Dehydroergosterol structural organization in aqueous medium and in a model system of membranes. Biophys J 1997;72:2226–2236. [PubMed: 9129825]
97. Yeagle PL, Bensen J, Greco M, Arena C. Cholesterol behavior in human serum lipoproteins. Biochem 1982;21:1249–1254. [PubMed: 7074081]
98. Schroeder F, Goh EH. Regulation of very low density lipoprotein interior core lipid physicochemical properties. J Biol Chem 1979;254:2464–2470. [PubMed: 218938]
99. Schroeder F, Goh EH, Heimberg M. Investigation of the surface structure of the very low density lipoprotein using fluorescence probes. FEBS Lett 1979;97:233–236. [PubMed: 216583]
100. Bergeron RJ, Scott J. Fluorescent lipoprotein probe. Anal Chem 1982;119:128–134.
101. Bergeron RJ, Scott J. Cholestatriene and ergostatetraene as in vivo and in vitro membrane and lipoprotein probes. J Lipid Res 1982;23:391–404. [PubMed: 7077153]
102. Schroeder F, Gallegos AM, Atshaves BP, McIntosh A, Petrescu AD, Huang H, Chao H, Yang H, Frolov A, Kier AB. Recent advances in membrane microdomains: rafts, caveolae and intracellular cholesterol trafficking. Exp Biol Med 2001;226:873–890.
103. Stolowich NJ, Petrescu AD, Huang H, Martin G, Scott AI, Schroeder F. Sterol carrier protein-2: structure reveals function. Cell Mol Life Sci 2002;59:193–212. [PubMed: 11915938]
104. Colles SM, Woodford JK, Moncecchi D, Myers-Payne SC, McLean LR, Billheimer JT, Schroeder F. Cholesterol interactions with recombinant human sterol carrier protein-2. Lipids 1995;30:795–804. [PubMed: 8577222]

105. Nemecz G, Schroeder F. Selective binding of cholesterol by recombinant fatty acid-binding proteins. J Biol Chem 1991;266:17180–17186. [PubMed: 1894612]

106. Schroeder F, Dempsey ME, Fischer RT. Sterol and squalene carrier protein interactions with fluorescent delta 5,7,9(11)-cholestatrien-3 beta-ol. J Biol Chem 1985;260:2904–2911. [PubMed: 3972810]

107. Schroeder, F.; Butko, P.; Nemecz, G.; Jefferson, JR.; Powell, D.; Rymaszewski, Z.; Dempsey, ME.; Kukowska-Latallo, J.; Lowe, JB. Sterol carrier protein: a ubiquitous protein in search of a function. In: Verna, R.; Blumenthal, R.; Frati, L., editors. Bioengineered Molecules: Basic and Clinical Aspects. Raven Press; New York, NY: 1989. p. 29-45.

108. Kubelt JK, Muller P, Wustner D, Hermann A. Rapid transbilayer movement of the fluorescent sterol dehydroergosterol in lipid membranes. Biophys J 2002;83:1525–1534. [PubMed: 12202377]

109. Raghuraman H, Chattopadhyay A. Interaction of mellitin with membrane cholesterol: a fluroescence approach. Biophys J 2004;87:2419–2432. [PubMed: 15454440]

110. Schroeder F, Nemecz G, Gratton E, Barenholz Y, Thompson TE. Fluorescence properties of cholestatrienol in phosphatidylcholine bilayer vesicles. Biophys Chem 1988;32:57–72. [PubMed: 3233314]

111. Schroeder F, Barenholz Y, Gratton E, Thompson TE. A fluorescence study of dehydroergosterol in phosphatidylcholine bilayer vesicles. Biochemistry 1987;26:2441–2448. [PubMed: 3607026]

112. Schroeder, F.; Nemecz, G.; Barenholz, Y.; Gratton, E.; Thompson, TE. Cholestatrienol Time Resolved Fluorescence in Phosphatidylcholine Bilayers. In: Lakowicz, JR.; Eftink, M.; Wampler, J., editors. Time Resolved Laser Spectroscopy in Biochemistry. 909. SPIE Press; 1988. p. 457-465.

113. Bar LK, Chong PLG, Barenholz Y, Thompson TE. Spontaneous transfer between phospholipid bilayers of dehydroergosterol, a fluorescent sterol analog. Biochim Biophys Acta 1989;983:109–112. [PubMed: 2758045]

114. Chong PL, Liu F, Wang MM, Truong K, Sugar IP, Brown RE. Fluorescence evidence for cholesterol regular distribution in phosphatidylcholine and in sphingomyelin lipid bilayers. J Fluorescence 1996;6:221–224.

115. Chong PLG. Evidence for regular distribution of sterols in liquid crystalline phosphatidylcholine bilayers. Proc Natl Acad Sci 1994;91:10069–10073. [PubMed: 7937839]

116. Liu F, Sugar IP, Chong PL. Cholesterol and ergosterol superlattices in three-component liquid crystalline lipid bilayers as revealed by dehydroergosterol fluorescence. Biophys J 1997;72:2243–2254. [PubMed: 9129827]

117. Nemecz G, Fontaine RN, Schroeder F. A fluorescence and radiolabel study of sterol exchange between membranes. Biochim Biophys Acta 1988;943:511–521. [PubMed: 3415992]

118. Butko P, Hapala I, Nemecz G, Schroeder F. Sterol domains in phospholipid membranes: dehydroergosterol polarization measures molecular sterol transfer. J Biochem Biophys Meth 1992;24:15–37. [PubMed: 1560178]

119. Nemecz G, Schroeder F. Time-resolved fluorescence investigation of membrane cholesterol heterogeneity and exchange. Biochemistry 1988;27:7740–7749. [PubMed: 3207705]

120. Schroeder F, Nemecz G. Interaction of sphingomyelins and phosphatidylcholines with fluorescent dehydroergosterol. Biochemistry 1989;28:5992–6000. [PubMed: 2775747]

121. Butko P, Hapala I, Scallen TJ, Schroeder F. Acidic phospholipids strikingly potentiate sterol carrier protein 2 mediated intermembrane sterol transfer. Biochemistry 1990;29:4070–4077. [PubMed: 2361131]

122. Hapala I, Kavecansky J, Butko P, Scallen TJ, Joiner C, Schroeder F. Regulation of membrane cholesterol domains by sterol carrier protein-2. Biochemistry 1994;33:7682–7690. [PubMed: 8011635]

123. Hapala I, Butko P, Schroeder F. Role of acidic phospholipids in intermembrane sterol transfer. Chem Phys Lipids 1990;56:37–47. [PubMed: 2091835]

124. Schroeder F, Butko P, Hapala I, Scallen TJ. Intermembrane cholesterol transfer: role of sterol carrier proteins and phosphatidylserine. Lipids 1990;25:669–674. [PubMed: 2280670]

125. Huang H, Ball JA, Billheimer JT, Schroeder F. The sterol carrier protein-2 amino terminus: a membrane interaction domain. Biochemistry 1999;38:13231–13243. [PubMed: 10529196]

126. Huang H, Ball JA, Billheimer JT, Schroeder F. Interaction of the N-terminus of sterol carrier protein-2 with membranes: role of membrane curvature. Biochem J 1999;344:593–603. [PubMed: 10567245]

127. Huang H, Gallegos A, Zhou M, Ball JM, Schroeder F. Role of sterol carrier protein-2 N-terminal membrane binding domain in sterol transfer. Biochemistry 2002;41:12149–12162. [PubMed: 12356316]

128. Matyash V, Geier C, Henske A, Mukherjee S, Hirsh D, Thiele C, Grant B, Maxfield FR, Kurzchalia TV. Distribution and transport of cholesterol in Caenorhabditis elegans. Mol Biol Cell 2001;12:1725–1736. [PubMed: 11408580]

129. Schoer J, Gallegos A, Starodub O, Petrescu A, Roths JB, Kier AB, Schroeder F. Lysosomal membrane cholesterol dynamics: role of sterol carrier protein-2 gene products. Biochemistry 2000;39:7662–7677. [PubMed: 10869172]

130. Chao H, Billheimer JT, Kier AB, Schroeder F. Microsomal long chain fatty acyl-CoA transacylation: differential effect of sterol carrier protein-2. Biochim Biophys Acta 1999;1439:371–383. [PubMed: 10498408]

131. Deliconstantinos G. Effect of rat serum albumin-cholesterol on the physcial properties of biomembranes. Biochem Intern 1987;45:467–474.

132. Deliconstantinos G. Evidence for the existence of non-esterified cholesterol carried by albumin in rat serum. Atherosclerosis 1986;61:67–75. [PubMed: 3015157]

133. Fielding CJ, Moser K. Evidence for the separation of albumin- and apo A−/−dependent mechanisms of cholesterol efflux from cultured fibroblasts into human plasma. J Biol Chem 1982;257:10955–10960. [PubMed: 6809760]

134. Zhao Y, Marcel YL. Serum albumin is a significant intermediate in cholesterol transfer between cells and lipoproteins. Biochemistry 1996;35:7174–7180. [PubMed: 8679545]

135. Gallegos AM, Atshaves BP, Storey S, McIntosh A, Petrescu AD, Schroeder F. Sterol carrier protein-2 expression alters plasma membrane lipid distribution and cholesterol dynamics. Biochemistry 2001;40:6493–6506. [PubMed: 11371213]

136. Gallegos AM, McIntosh AL, Atshaves BP, Schroeder F. Structure and cholesterol domain dynamics of an enriched caveolae/raft isolate. Biochem J 2004;382:451–461. [PubMed: 15149285]

137. Gallegos AM, McIntosh AL, Kier AB, Schroeder F. Membrane domain distributions: Analysis of fluorescent sterol exchange kinetics. Current Analytical Chemistry 2008;4:1–7.

138. Woodford JK, Colles SM, Myers-Payne S, Billheimer JT, Schroeder F. Sterol carrier protein-2 stimulates intermembrane sterol transfer by direct membrane interaction. Chem Phys Lipids 1995;76:73–84. [PubMed: 7788802]

139. Woodford JK, Jefferson JR, Wood WG, Hubbell T, Schroeder F. Expression of liver fatty acid binding protein alters membrane lipid composition and structure in transfected L-cell fibroblasts. Biochim Biophys Acta 1993;1145:257–265. [PubMed: 8431458]

140. Woodford JK, Hapala I, Jefferson JR, Knittel JJ, Kavecansky J, Powell D, Scallen TJ, Schroeder F. Mechanistic studies of sterol carrier protein-2 effects on L- cell fibroblast plasma membrane sterol domains. Biochim Biophys Acta 1994;1189:52–60. [PubMed: 8305459]

141. Woodford JK, Behnke WD, Schroeder F. Liver fatty acid binding protein enhances sterol transfer by membrane interaction. Mol Cell Biochem 1995;152:51–62. [PubMed: 8609911]

142. Gallegos AM, Schoer J, Starodub O, Kier AB, Billheimer JT, Schroeder F. A potential role for sterol carrier protein-2 in cholesterol transfer to mitochondria. Chem Phys Lipids 2000;105:9–29. [PubMed: 10727111]

143. Petrescu AD, Gallegos AM, Okamura Y, Strauss IJF, Schroeder F. Steroidogenic acute regulatory protein binds cholesterol and modulaes mitochondrial membrane sterol domain dynamics. J Biol Chem 2001;276:36970–36982. [PubMed: 11489878]

144. Schroeder F, Nemecz G, Wood WG, Joiner C, Morrot G, Ayraut-Jarrier M, Devaux PF. Transmembrane distribution of sterol in the human eurythrocyte. Biochim Biophys Acta 1991;1066:183–192. [PubMed: 1854783]

145. Wood WG, Schroeder F, Hogy L, Rao AM, Nemecz G. Asymmetric distribution of a fluorescent sterol in synaptic plasma membranes: effects of chronic ethanol consumption. Biochim Biophys Acta 1990;1025:243–246. [PubMed: 2364080]

146. Schroeder F, Kier AB, Sweet WD. Role of polyunsaturated fatty acids and lipid peroxidation in LM fibroblast plasma membrane structure. Arch Biochem Biophys 1990;276:55–64. [PubMed: 2297230]

147. Sweet WD, Schroeder F. Polyunsaturated fatty acids alter sterol transbilayer domains in LM fibroblast plasma membrane. FEBS Lett 1988;229:188–192. [PubMed: 2831087]

148. Hayashi H, Igbavboa U, Hamanaka H, Kobayashi M, Fujita SC, Wood WG, Yanagisawa K. Cholesterol is increased in the exofacial leaflet of plasma membranes of human apoE4 knock-in mice. Neuroreport 2002;13:383–386. [PubMed: 11930145]

149. Igbavboa U, Avdulov NA, Schroeder F, Wood WG. Increasing age alters transbilayer fluidity and cholesterol asymmetry in synaptic plasma membranes of mice. J Neurochem 1996;66:1717–1725. [PubMed: 8627330]

150. Igbavboa U, Avdulov NA, Chochina SV, Wood WG. Transbilayer distribution of cholesterol is modified in brain synaptic plasma membranes of knockout mice deficient in the LDL receptor, apoE, or both proteins. J Neurochem 1997;69:1661–1667. [PubMed: 9326295]

151. Wood WG, Eckert GP, Igbavboa U, Mueller WE. Amyloid beta-protein interactions with membranes and cholesterol: causes or casualties of Alzheimer's disease. Biochim Biophys Acta 2003;1610:281–290. [PubMed: 12648781]

152. Brasaemle DL, Robertson RD, Attie AD. Transbilayer movement of cholesterol in the human eurythrocyte membrane. J Lipid Res 1988;29:481–489. [PubMed: 3392465]

153. Schroeder, F.; Sweet, WD. The role of membrane lipid and structure asymmetry on transport systems. In: Jorgensen, PL.; Verna, R., editors. Advances in Biotechnology of Membrane Ion Transport. 51. Serono Symposia; New York, NY: 1988. p. 183-195.

154. Sweet WD, Wood WG, Schroeder F. Charged anesthetics selectively alter plasma membrane order. Biochemistry 1987;26:2828–2835. [PubMed: 3038166]

155. Sweet WD, Schroeder F. Plasma membrane lipid composition modulates action of anesthetics. Biochim Biophys Acta 1986;861:53–61. [PubMed: 3756155]

156. Sweet, WD.; Schroeder, F. Lipid domains and enzyme activity. In: Aloia, RC.; Cirtain, CC.; Gordon, LM., editors. Advances in Membrane Fluidity: Lipid Domains and the Relationship to Membrane Function. Alan R. Liss, Inc.; New York, NY: 1988. p. 17-42.

157. Wood WG, Gorka C, Schroeder F. Acute and chronic effects of ethanol on transbilayer membrane domains. J Neurochem 1989;52:1925–1930. [PubMed: 2723646]

158. Wood, WG.; Rao, AM.; Schroeder, F.; Igbavboa, U. Membrane cholesterol and ethanol: domains, kinetics, and protein function. In: Alling, C.; Diamond, I.; Leslie, SW.; Sun, GY.; Wood, WG., editors. Alcohol, Cell Membranes, and Signal Transduction in Brain. Plenum Press; New York: 1993. p. 13-32.

159. Wood, WG.; Schroeder, F.; Rao, AM.; Igbavboa, U.; Avdulov, NA. Membranes and ethanol: lipid domains and lipid protein interactions. In: Dietrich, R.; Erwin, VG., editors. Pharmacological Effects of Ethanol on the Nervous System. CRC Press; Boca Raton, FL: 1996. p. 13-27.

160. Wustner D, Herrmann A, Hao M, Maxfield FR. Rapid nonvesicular transport of sterol between the plasma membrane domains of polarized hepatic cells. J Biol Chem 2002;277:30325–30336. [PubMed: 12050151]

161. Colles SM, Wood WG, Myers-Payne SC, Igbavboa U, Avdulov NA, Joseph J, Schroeder F. Structure and Polarity of Mouse Brain Synaptic Plasma Membrane:Effects of Ethanol *in vitro* and *in vivo*. Biochemistry 1995;34:5945–5959. [PubMed: 7727452]

162. Schroeder F, Morrison WJ, Gorka C, Wood WG. Transbilayer effects of ethanol on fluidity of brain membrane leaflets. Biochim Biophys Acta 1988;946:85–94. [PubMed: 3207734]

163. Schroeder F, Gorka C, Williamson LS, Wood WG. The influence of dolichols on fluidity of mouse synaptic plasma membranes. Biochim Biophys Acta 1987;902:385–393. [PubMed: 3040098]

164. Wood WG, Lahiri S, Gorka C, Armbrecht HJ, Strong R. *In vitro* effects of ethanol on erythrocyte membrane fluidity of alcoholic patients: an electron spin resonance study. Alcoholism Clin Exp Res 1987;11:332–335.

165. Wood WG, Chochina SV, Igbavboa U, O'Hare EO, Schroeder F, Cleary JP, Avdulov NA. Amyloid B alters brain synaptic plasma membrane lipid structure and lipid-protein interaction. J Neurochem 1997;68:2086–2091. [PubMed: 9109536]

166. Wood WG, Schroeder F, Avdulov NA, Chochina SV, Igbavboa U. Recent advances in brain cholesterol dynamics: transport, domains, and Alzheimer's disease. Lipids 1999;34:225–234. [PubMed: 10230715]

167. Harris RA, Schroeder F. Effects of barbiturates and ethanol on the physical properties of brain membranes. J Pharm Exp Ther 1982;223:424–431.

168. Harris RA, Schroeder F. Ethanol and the physical properties of brain membranes: fluorescence studies. Mol Pharmacol 1981;20:128–137. [PubMed: 7290080]

169. Schroeder F, Goetz I, Roberts E. Age-related alterations in cultured human fibroblast membrane structure and function. Mech Ageing Dev 1984;25:365–389. [PubMed: 6330463]

170. Schroeder F, Goetz IE, Roberts E. Membrane anomalies in Huntington's disease fibroblasts. J Neurochem 1984;43:526–539. [PubMed: 6330302]

171. Schroeder F. Role of membrane lipid asymmetry in aging. [Review]. Neurobiol Aging 1984;5:323–333. [PubMed: 6397694]

172. Atshaves BP, Gallegos A, McIntosh AL, Kier AB, Schroeder F. Sterol carrier protein-2 selectively alters lipid composition and cholesterol dynamics of caveolae/lipid raft vs non-raft domains in L-cell fibroblast plasma membranes. Biochemistry 2003;42:14583–14598. [PubMed: 14661971]

173. Gallegos AM, Atshaves BP, Storey SM, Starodub O, Petrescu AD, Huang H, McIntosh A, Martin G, Chao H, Kier AB, Schroeder F. Gene structure, intracellular localization, and functional roles of sterol carrier protein-2. Prog Lipid Res 2001;40:498–563. [PubMed: 11591437]

174. Mukherjee S, Zha X, Tabas I, Maxfield FR. Cholesterol distribution in living cells:fluorescence imaging using dehydroergosterol as a fluorescent cholesterol analog. Biophys J 1998;75:1915–1925. [PubMed: 9746532]

175. Wustner D, Mondal M, Tabas I, Maxfield FR. Direct observation of rapid internalization and intracellular transport of sterol by macrophage foam cells. Traffic 2005;6:396–412. [PubMed: 15813750]

176. Wustner D, Mondal M, Huang A, Maxfield FR. Different routes of transport for high density lipoprotein and its associated free sterol in polarized hepatic cells. J Lipid Res 2004;45:427–437. [PubMed: 14679167]

177. Puglielli L, Rigotti A, Amigo L, Nunez L, Greco AV, Santos MJ, Nervi F. Modulation on intrahepatic cholesterol trafficking: Evidence by *in vivo* antisense treatment for the involvement of sterol carrier protein-2 in newly synthesized cholesterol transfer into bile. Biochem J 1996;317:681–687. [PubMed: 8760350]

178. Amigo L, Zanlungo S, Miquel JF, Glick JM, Hyogo H, Cohen DE, Rigotti A, Nervi F. Hepatic overexpression of sterol carrier protein-2 inhibits VLDL production and reciprocally enhances biliary lipid secretion. J Lipid Res 2003;44:399–407. [PubMed: 12576522]

179. Zanlungo S, Amigo L, Mendoza H, Glick J, Rodriguez A, Kozarsky K, Miquel JF, Rigotti A, Nervi F. Overexpression of sterol carrier protein-2 in mice leads to increased hepatic cholesterol content and enterohepatic circulation of bile acids. Gastroenterology 2000;118:135.A1165

180. Fuchs M, Hafer A, Muench C, Kannenberg F, Teichmann S, Scheibner J, Stange EF, Seedorf U. Disruption of the sterol carrier protein 2 gene in mice impairs biliary lipid and hepatic cholesterol metabolism. J Biol Chem 2001;276:48058–48065. [PubMed: 11673458]

181. Muench C, Hafer A, Katzberg N, Scheibner J, Stange EF, Seedorf U, Fuchs M. Relevance of the sterol carrier protein-2 gene for bile acid synthesis and gallstone formation in genetically susceptible mice. Gastroenterology 2000;118(4 Part 1 Supplement 2)Ref Type: Abstract

182. Atshaves BP, McIntosh AL, Payne HR, Gallegos AM, Landrock K, Maeda N, Kier AB, Schroeder F. Sterol carrier protein-2/sterol carrier protein-x gene ablation alters lipid raft domains in primary cultured mouse hepatocytes. J Lipid Res 2007;48:2193–2211. [PubMed: 17609524]

183. Atshaves BP, McIntosh AL, Landrock D, Payne HR, Mackie J, Maeda N, Ball JM, Schroeder F, Kier AB. Effect of SCP-x gene ablation on branched-chain fatty acid metabolism. Am J Physiol 2007;292:939–951.

184. Martin GG, Danneberg H, Kumar LS, Atshaves BP, Erol E, Bader M, Schroeder F, Binas B. Decreased liver fatty acid binding capacity and altered liver lipid distribution in mice lacking the liver fatty acid binding protein (L-FABP) gene. J Biol Chem 2003;278:21429–21438. [PubMed: 12670956]

185. Martin GG, Huang H, Atshaves BP, Binas B, Schroeder F. Ablation of the liver fatty acid binding protein gene decreases fatty acyl CoA binding capacity and alters fatty acyl CoA pool distribution in mouse liver. Biochem 2003;42:11520–11532. [PubMed: 14516204]

186. Martin GG, Atshaves BP, McIntosh AL, Mackie JT, Kier AB, Schroeder F. Liver fatty acid binding protein (L-FABP) gene ablation alters liver bile acid metabolism in male mice. Biochem J 2005;391:549–560. [PubMed: 15984932]

187. Martin GG, Atshaves BP, McIntosh AL, Mackie JT, Kier AB, Schroeder F. Liver fatty acid binding protein (L-FABP) gene ablation potentiates hepatic cholesterol accumulation in cholesterol-fed female mice. Am J Physiol 2006;290:G36–G48.

188. Martin GG, Atshaves BP, McIntosh AL, Mackie JT, Kier AB, Schroeder F. Increased age-dependent obesity in liver fatty acid binding protein gene-ablated mice. J Nutrition. 2008(submitted)

189. Martin GG, Atshaves BP, McIntosh AL, Payne HR, Mackie JT, Kier AB, Schroeder F. Liver fatty acid binding protein gene ablation enhances age-dependent obesity in male mice. Molecular and Cellular Biochemistry. 2008(submitted)

190. Puglielli L, Rigotti A, Greco AV, Santos MJ, Nervi F. Sterol carrier protein-2 is involved in cholesterol transfer from the endoplasmic reticulum to the plasma membrane in human fibroblasts. J Biol Chem 1995;270:18723–18726. [PubMed: 7642518]

191. Moncecchi DM, Murphy EJ, Prows DR, Schroeder F. Sterol carrier protein-2 expression in mouse L-cell fibroblasts alters cholesterol uptake. Biochim Biophys Acta 1996;1302:110–116. [PubMed: 8695660]

192. Murphy EJ, Schroeder F. Sterol carrier protein-2 mediated cholesterol esterification in transfected L-cell fibroblasts. Biochim Biophys Acta 1997;1345:283–292. [PubMed: 9150248]

193. Jefferson JR, Powell DM, Rymaszewski Z, Kukowska-Latallo J, Schroeder F. Altered membrane structure in transfected mouse L-Cell fibroblasts expressing rat liver fatty acid-binding protein. J Biol Chem 1990;265:11062–11068. [PubMed: 2358452]

194. Jefferson JR, Slotte JP, Nemecz G, Pastuszyn A, Scallen TJ, Schroeder F. Intracellular sterol distribution in transfected mouse L-cell fibroblasts expressing rat liver fatty acid binding protein. J Biol Chem 1991;266:5486–5496. [PubMed: 2005092]

195. Baum CL, Reschly EJ, Gayen AK, Groh ME, Schadick K. Sterol carrier protein-2 overexpression enhances sterol cycling and inhibits cholesterol ester synthesis and high density lipoprotein cholesterol secretion. J Biol Chem 1997;272:6490–6498. [PubMed: 9045674]

196. Atshaves BP, Jefferson JR, McIntosh AL, McCann BM, Landrock K, Kier AB, Schroeder F. Effect of sterol carrier protein-2 expression on sphingolipid distribution in plasma membrane lipid rafts/caveolae. Lipids 2007;42:871–884. [PubMed: 17680294]

197. Kriska T, Levchenko VV, Korytowski W, Atshaves BP, Schroeder F, Girotti AW. Hypersensitivity of sterol carrier protein-2 overexpressing hepatoma cells to lethal peroxidative damage induced by an exogenous cholesterol hydroperoxide. J Biol Chem 2006;281:23643–23651. [PubMed: 16772292]

198. Roff CF, Pastuszyn A, Strauss JFI, Billheimer JT, Vanier MT, Brady RO, Scallen TJ, Pentchev PG. Deficiencies in sex-regulated expression and levels of two hepatic sterol carrier proteins in a murine model of Niemann-Pick type C disease. J Biol Chem 1992;267:15902–15908. [PubMed: 1639819]

199. Kobayashi T, Beuchat MH, Lindsay M, Frias S, Palmiter RD, Sakuraba H, Parton RG, Gruenberg J. Late endosomal membranes rich in lysobisphosphatidic acid regulate cholesterol transport. Nature Cell Biology 1999;1:113–118.

200. Zhou M, Parr RD, Petrescu AD, Payne HR, Atshaves BP, Kier AB, Ball JA, Schroeder F. Sterol carrier protein-2 directly interacts with caveolin-1 in vitro and in vivo. Biochem 2004;43:7288–7306. [PubMed: 15182174]

201. Parr RD, Martin GG, Hostetler HA, Schroeder ME, Mir KD, Kier AB, Ball JM, Schroeder F. A new N-terminal recognition domain in caveolin-1 interacts with sterol carrier protein-2 (SCP-2). Biochemistry 2007;46:8301–8314. [PubMed: 17580960]

202. Duncan, MJ.; Abraham, SN. Lipid Raft Mediated Entry of Bacteria into Host Cells. In: Lisanti, MP.; Frank, PG., editors. Caveolae and Lipid Rafts: Roles in Signal Transduction and the Pathogenesis of Human Disease. 36. Elsevier Academic Press; San Diego: 2005. p. 79-88.

203. Zhang W, McIntosh A, Xu H, Wu D, Gruninger T, Atshaves BP, Liu JCS, Schroeder F. Structural analysis of sterol distribution in the plasma membrane of living cells. Biochemistry 2005;44:2864–2984. [PubMed: 15723530]

204. McIntosh, A.; Atshaves, BP.; Huang, H.; Gallegos, AM.; Kier, AB.; Schroeder, F.; Xu, H.; Zhang, W.; Liu, S. Multiphoton laser scanning microscopy and spatial analysis of dehydroergosterol distributions on plasma membranes of living cells. In: McIntosh, T., editor. Lipid Rafts. Humana Press Inc.; Totowa, N.J.: 2007. p. 85-105.

205. Schroeder F, Butko P, Nemecz G, Scallen TJ. Interaction of fluorescent delta 5,7,9(11),22-ergostatetraen-3β-ol with sterol carrier protein-2. J Biol Chem 1990;265:151–157. [PubMed: 2294101]

206. Denk W, Strickler JH, Webb WW. Two-photon laser scanning fluorescence microscopy. Science 1990;2:73–76. [PubMed: 2321027]

207. Williams RM, Zipfel WR, Webb WW. Multiphoton microscopy in biological research. Current Opinion in Chemical Biology 2001;5:603–608. [PubMed: 11578936]

208. Maiti S, Shear JB, Williams RM, Zipfel WR, Webb WW. Measuring serotonin distribution in live cells with three-photon excitation. Science 1997;275:530–532. [PubMed: 8999797]

209. Williams RM, Shear JB, Zipfel WRMS, Webb WW. Mucosal mast cell secretion processes imaged using three-photon microscopy of 5-hydroxytryptamine autofluorescence. Biophysical Journal 1999;76:1835–1846. [PubMed: 10096882]

210. Wustner D. Improved visualization and quantitative analysis of fluorescent membrane sterol in polarized hepatic cells. J Microscopy 2005;220:47–64.

211. Wustner D. Plasma membrane sterol distribution resembles the surface topography of living cells. Mol Biol Cell 2007;18:211–228. [PubMed: 17065557]

212. Mobius W, Ohno-Iwashita Y, van Donselaar E, Oorschot VMJ, Shimada Y, Fujimoto T, Heijnen HFG, Geuze HJ, Slot JW. Immunoelectron microscopic localization of cholesterol using biotinylated and non-cytolytic perfringolysin O. J Histochem Cytochem 2002;50:43–55. [PubMed: 11748293]

213. Waheed AA, Shimada Y, Heijnen HFG, Nakamura M, Inomata M, Hayashi M, Iwashita S, Slot JW, Ohno-Iwashita Y. Selective binding of perfringolysin O derivative to cholesterol-rich membrane microdomains (rafts). Proc Natl Acad Sci U S A 2001;98:4926–4931. [PubMed: 11309501]

214. Sankaram MB, Thompson TE. Cholesterol-induced fluid-phase immiscibility in membranes. Proc Natl Acad Sci 1991;88:8689–8690.

215. Schroeder R, London E, Brown D. Interactions between saturated acyl chains confer detergent resistance on lipids and glycosylphosphatidylinositol (GPI)-anchored proteins: GPI-anchored proteins in liposomes and cells show similar behavior. Proc Natl Acad Sci 1994;91:12130–12134. [PubMed: 7991596]

216. Anderson RG. Caveolae: where incoming and outgoing messengers meet. [Review] [68 refs]. Proceedings of the National Academy of Sciences of the United States of America 1993;90:10909–10913. [PubMed: 8248193]

217. Mukherjee S, Maxfield FR. Membrane domains. Annu Rev Cell Biol 2004;20:839–866.

218. Babitt J, Trigatti B, Rigotti A, Smart EJ, Anderson RGW, Xu S, Krieger M. Murine SR-BI, a high density lipoprotein receptor that mediates selective lipid uptake, is *N*-Glycosylated and fatty acylated and colocalizes with plasma membrane caveolae. J Biol Chem 1997;272:13242–13249. [PubMed: 9148942]

219. Barlage S, Boettcher D, Boettcher A, Dada A, Schmitz G. High density lipoprotein modulates platelet function. Cytometry Part A: J Internat Soc Anal Cytol 2006;69A:196–199.

220. Chao WT, Tsai SH, Lin YC, Lin WW, Yang VC. Cellular localization and interaction of ABCA1 and caveolin-1 in aortic endothelial cells after HDL incubation. Biochem Biophys Res Commun 2005;332:743–749. [PubMed: 15907796]

221. Connelly MA, Williams DL. Scavenger receptor B1: A scavenger receptor with a mission to transport high density lipoprotein lipids. Cur Opin Lipidology 2004;15:287–295.

222. Demeule M, Jodoin J, Gingras D, Beliveau R. FEBS Lett 2000;466:219–224. [PubMed: 10682831]

223. Drobnik W, Borsukova H, Bottcher A, Pfeiffer A, Liebisch G, Schutz GJ, Schindler H, Schmitz G. Apo AI/ABCA1-dependent and HDL3-mediated lipid efflux from compositionally distinct cholesterol-based microdomains. Traffic 2002;3:268–278. [PubMed: 11929608]

224. Duong M, Collins HL, Jin W, Zanotti I, Favari E, Rothblat G. Relative contributions of ABCA1 and SR-BI to cholesterol efflux to serum from fibroblasts and macrophages. Arterioscler Thromb Vasc Biol 2006;26:541–547. [PubMed: 16410457]

225. Graf GA, Connell PM, van der Westhuyzen DR, Smart EJ. The class B, Type 1 scavenger receptor promotes the selective uptake of high density lipoprotein cholesterol into caveolae. J Biol Chem 1999;274:12034–12048.

226. Hinrichs JWJ, Klappe K, Hummel I, Kok JW. ATP-binding casette transporters are enriched in non-caveolar detergent insoluble glycosphingolipid-enriched membrane domains (DIGs) in human multidrug resistant cancer cells. J Biol Chem 2004;279:5734–5738. [PubMed: 14627714]

227. Jessup W, Gelissen I, Gaus K, Kritharides L. Roles of ATP binding cassette transporters A1 and G1, scavenger receptor BI and membrane lipid domains in cholesterol export from macrophages. Curr Opin Lipidol 2006;17:247–267. [PubMed: 16680029]

228. Kamau SW, Kramer SD, Gunthert M, Wunderlich-Allenspach H. Effect of the modulation of the membrane lipid composition on the localization and function of P-glycoprotein in MDR1-MDCK cells. In Vitro Cell Devel Biol 2005;41:207–216.

229. Lavie Y, Fiucci G, Liscovitch M. J Biol Chem 1998;273:3280–3283.

230. Luker GD, Pica CM, Kumar AS, Covey DF, Piwnica-Worms D. Effect of cholesterol and enantiomeric cholesterol on P-glycoprotein localization and function in low density membrane domains. Biochemistry 2000;39:7651–7661. [PubMed: 10869171]

231. Mendez AJ, Lin G, Wade DP, Lawn RM, Oram JF. Membrane lipid domains distinct from cholesterol/sphingomyelin-rich rafts are involved in the ABCA1-mediated lipid secretory pathway. J Biol Chem 2001;276:3158–3166. [PubMed: 11073951]

232. Nieland TJF, Chroni A, FitzGerald LM, Maliga Z, Zannis VI, Kirchhausen T, Krieger M. Cross-inhibition of SR-BI- and ABCA1-mediated cholesterol transport by the small molecules BLT-4 and glyburide. J Lipid Res 2004;45:1256–1265. [PubMed: 15102890]

233. Orso E, Broccardo C, Kaminski WE, Bottcher A, Liebisch G, Drobnik W, Gotz A, Chambenoit O, Diederich W, Langmann T, Spruss T, Luciani MF, Rothe G, Lackner KJ, Chimini G, Schmitz G. Transport of lipids from Golgi to plasma membrane is defective in Tangier disease patients and Abc1-deficient mice. Nature Genetics 2000;24:192–196. [PubMed: 10655069]

234. Parathath S, Connelly MA, Rieger RA, Klein SM, Abumrad NA, de la Llera-Moya M, Iden CR, Rothblat GH, Williams DL. Changes in plasma membrane properties and phosphatidylcholine subspecies of insect Sf9 cells due to expression of scavenger receptor class B, type 1, and CD36. J Biol Chem 2004;279:41310–41318. [PubMed: 15280390]

235. Peng Y, Akmentin W, Conneely MA, Lund-Katz S, Phillips MC, Williams DL. Scavenger receptor B1 (SR-B1) clustered on microvillar extensions suggests that this plasma membrane domain is a way station for cholesterol trafficking between cells and high density lipoprotein. Mol Biol Cell 2003;15:384–396. [PubMed: 14528013]

236. Rigotti A, Miettinen H, Kreiger M. The role of the high-density lipoprotein receptor SR-B1 in the lipid metabolism of endocrine and other tissues. Endocrine Rev 2003;23:357–383. [PubMed: 12788804]

237. Schmitz G, Kaminski WE, Orso E. ABC transporters in cellular lipid trafficking. Curr Opin Lipidol 2000;11:493–501. [PubMed: 11048892]

238. Smart, EJ. Caveolae and the regulation of cellular cholesterol homeostasis. In: Lisanti, MP.; Frank, PG., editors. Advances in Molecular and Cell Biology. 36. Elsevier B.V.; Amsterdam: 2005. p. 35

239. Yancey PG, Bortnick AE, Kellner-Weibel G, de la Llera-Moya M, Phillips MC, Rothblat GH. Importance of Different Pathways of Cellular Cholesterol Efflux. Arterioscler Thromb Vasc Biol 2003;23:712–719. [PubMed: 12615688]

240. Ehehalt R, Fullekrug J, Pohl J, Ring A, Herrmann T, Stremmel W. Translocation of long chain fatty acids across the plasma membrane--lipid rafts and fatty acid transport proteins. Mol Cell Biochem 2006;284:135–140. [PubMed: 16477381]

241. Koonen DPY, Glatz JFC, Bonen A, Luiken JJFP. Long-chain fatty acid uptake and FAT/CD36 translocation in heart and skeletal muscle. Biochim Biophys Acta 2006;1736:163–180. [PubMed: 16198626]

242. Ortegren U, Karlsson M, Blazic N, Blomqvist M, Nysrom FH, Gustavsson J, Fredman P, Stralfors P. Lipids and glycosphigolipids in caveolae and surrounding plasma membrane of primary rat adipocytes. Eur J Biochem 2007;271:2028–2036. [PubMed: 15128312]

243. Balbis ABG, Mounier C, Posner BI. Effect of insulin on caveolin-enriched membrane domains in rat liver. J Biol Chem 2004;279:39348–39357. [PubMed: 15252027]

244. Cohen AW, Combs TP, Scherer PE, Lisanti MP. Role of caveolin and caveolae in insulin signaling and diabetes. Am J Physiol Endocrinol Metab 2003;285:E1151–E1160. [PubMed: 14607781]

245. Elmendorf JS. Fluidity of insulin action. Mol Biotech 2004;27:127–138.

246. Ikonen E, Vainio S. Lipid microdomains and insulin resistance: is there a connection? Sci STKE 2005;pe3:1–3.

247. Ishikawa Y, Otsu K, Oshikawa J. Caveolin; different roles for insulin signal? Cell Signal 2005;17:1175–1182. [PubMed: 15913956]

248. Kumar AS, Xiao YP, Laipis PJ, Fletcher BS, Frost SC. Glucose deprivation enhances targeting of GLUT1 to lipid rafts in 3T3-L1 adipocytes. Am J Physiol Endocrinol Metab 2004;286:E568–E576. [PubMed: 14665446]

249. Matthews LC, Taggart MJ, Westwood M. Effect of cholesterol depletion on mitogenesis and survival: the role of caveolar and noncaveolar domains in insulin-like growth factor-mediated cellular function. Endocrinology 2005;146:5463–5473. [PubMed: 16166225]

250. Ortegren U, Yin L, Ost A, Karlsson H, Nystrom FH, Stralfors P. Separation and characterization of caveolae subclasses in the plasma membrane of primary adipocytes; segregation of specific proteins and functions. FEBS J 2006;273:3381–3392. [PubMed: 16803459]

251. Rauch MC, Ocampo ME, Bohle J, Amthauer R, Yanez AJ, Rodriguez-Gil JE, Slebe JC, Reyes JG, Concha II. Hexose transporters GLUT1 and GLUT3 are colocalized with hexokinase I in caveolae microdomains of rat spermatogenic cells. J Cell Physiol 2006;207:397–406. [PubMed: 16419038]

252. Saltiel AR, Pessin JE. Insulin signaling in microdomains of the plasma membrane. Traffic 2003;4:711–716. [PubMed: 14617354]

253. Syme CA, Zhang L, Bisello A. Caveolin-1 regulates cellular trafficking and function of the glucagon-like peptide 1 receptor. Mol Endocrinol 2006;20:3400–3411. [PubMed: 16931572]

254. Vainio S, Bykov I, Hermansson M, Jokitalo E, Somerharju P, Ikonen E. Defective insulin receptor activation and altered lipid rafts in Niemann-Pick type C disease hepatocytes. Biochem J 2005;391:465–472. [PubMed: 15943586]

255. Yamamoto M, Toyaf Y, Schwencke C, Lisanti MP, Myers MG, Iskikawa Y. Caveolin Is an Activator of Insulin Receptor Signaling. The Journal of Biological Chemistry 1998;273:26962–26968. [PubMed: 9756945]

256. Smart EJ, Graf GA, McNiven MA, Sessa WC, Engelman JA, Scherer PE, Okamoto T, Lisanti MP. Caveolins, Liquid-ordered domains, and signal transduction. Mol Cell Biol 1999;19:7289–7304. [PubMed: 10523618]

257. Liu P, Rudick M, Anderson RGW. Multiple functions of caveolin-1. J Biol Chem 2002;277:41295–41298. [PubMed: 12189159]

258. Stralfors, P. Insulin Signaling and Caveolae. In: Lisanti, MP.; Frank, PG., editors. Caveolae and Lipid Rafts: Roles in Signal Transduction and Human Disease. 36. Elsevier Academic Press; San Diego: 2005. p. 141-169.

259. Igarashi, J. eNOS regulation by sphingosine 1 phosphate and caveolin. In: Lisanti, MP.; Frank, PG., editors. Caveolae and Lipid Rafts: Roles in Signal Transduction and the Pathogenesis of Human Disease. Elsevier Academic Press; New York: 2005. p. 125-140.

260. Morris, R.; Cox, H.; Mombelli, E.; Quinn, P. Rafts, Little caves and large potholes: How lipid structure interacts with membrane proteins to create functionally diverse membrane environments. In: Quinn, P., editor. Subcellular Biochemistry: Membrane Dynamics and Domains. 37. Kluwer Academic/Plenum; New York: 2004. p. 35-118.

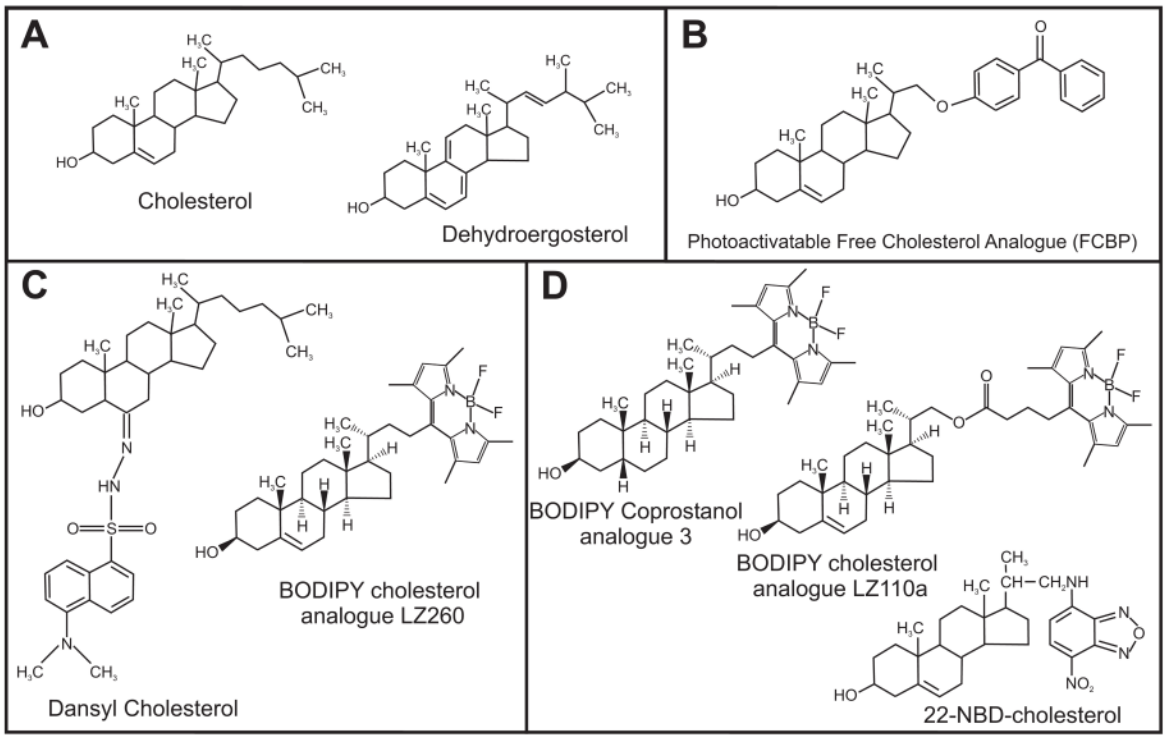


**Fig. 1. Structures of cholesterol and fluorescent cholesterol analogs**

**A.** Naturally-occurring sterols: cholesterol and fluorescent sterol dehydroergosterol (DHE); **B.** Photo-activatable cholesterol analog, (FCBP); **C.** Cholesterol-rich microdomain preferring cholesterol analogs: Dansyl-cholesterol, (DChol); BODIPY-cholesterol analog (LZ260); **D.** Cholesterol-poor microdomain preferring cholesterol analogs: BODIPY-coprostanol analog 3; BODIPY-cholesterol analog LZ110a; 22-NBD-cholesterol.

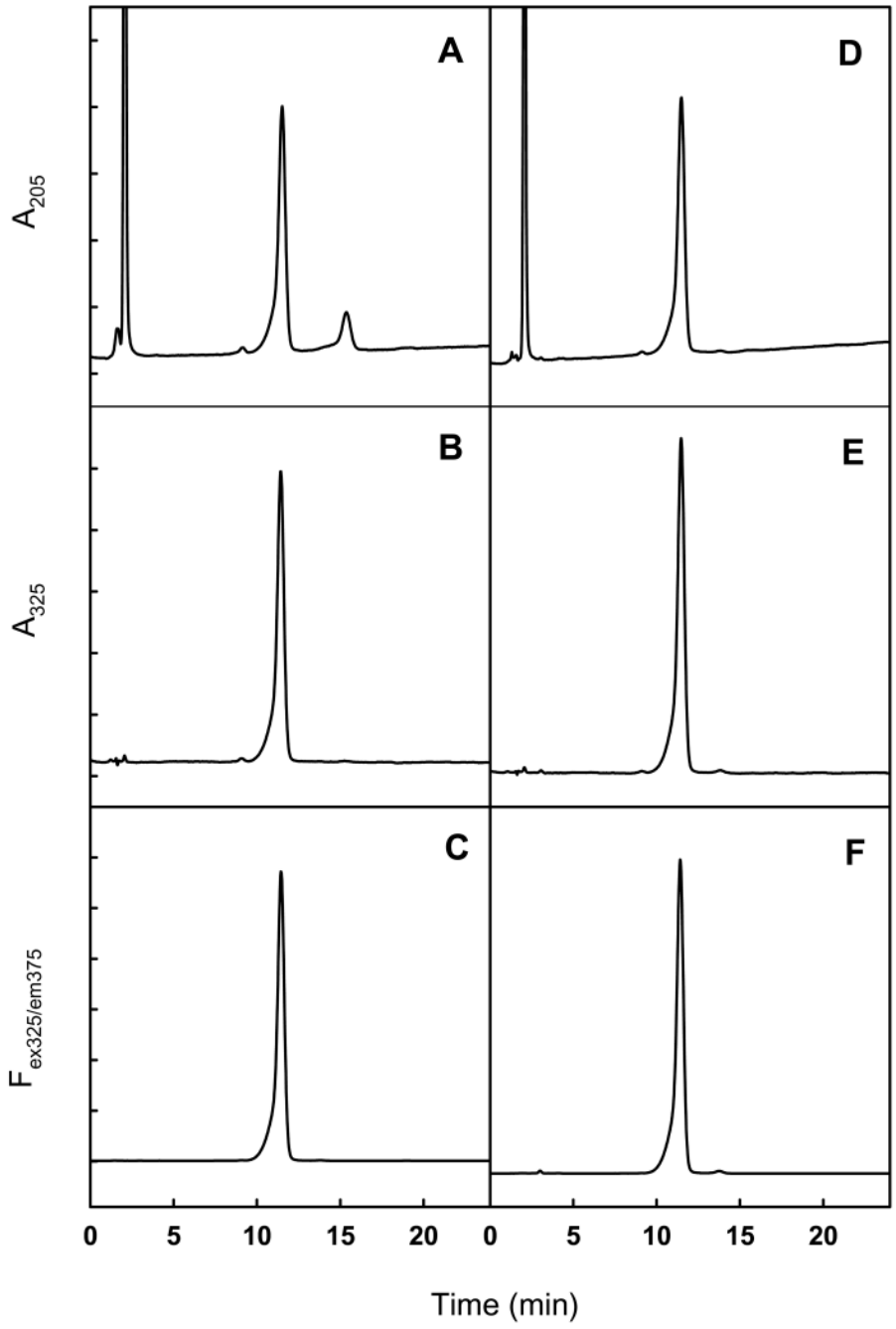


**Fig. 2. HPLC analysis of DHE**

**A-C.** DHE synthesized by established method as described in Methods. **D-F.** DHE synthesized by an improved method as described in Methods. Reversed phase HPLC was performed and elution of organic compounds was detected by absorbance at 205 nm **(A, D)**. Elution of DHE was specifically detected by absorbance at 325 nm **(B,E)** and by fluorescence emission at 375 nm upon excitation at 325 nm **(C,F)**. The peak with retention time at 11.75 min was due to DHE while that at 15.3 min was due to a non-fluorescent sterol.

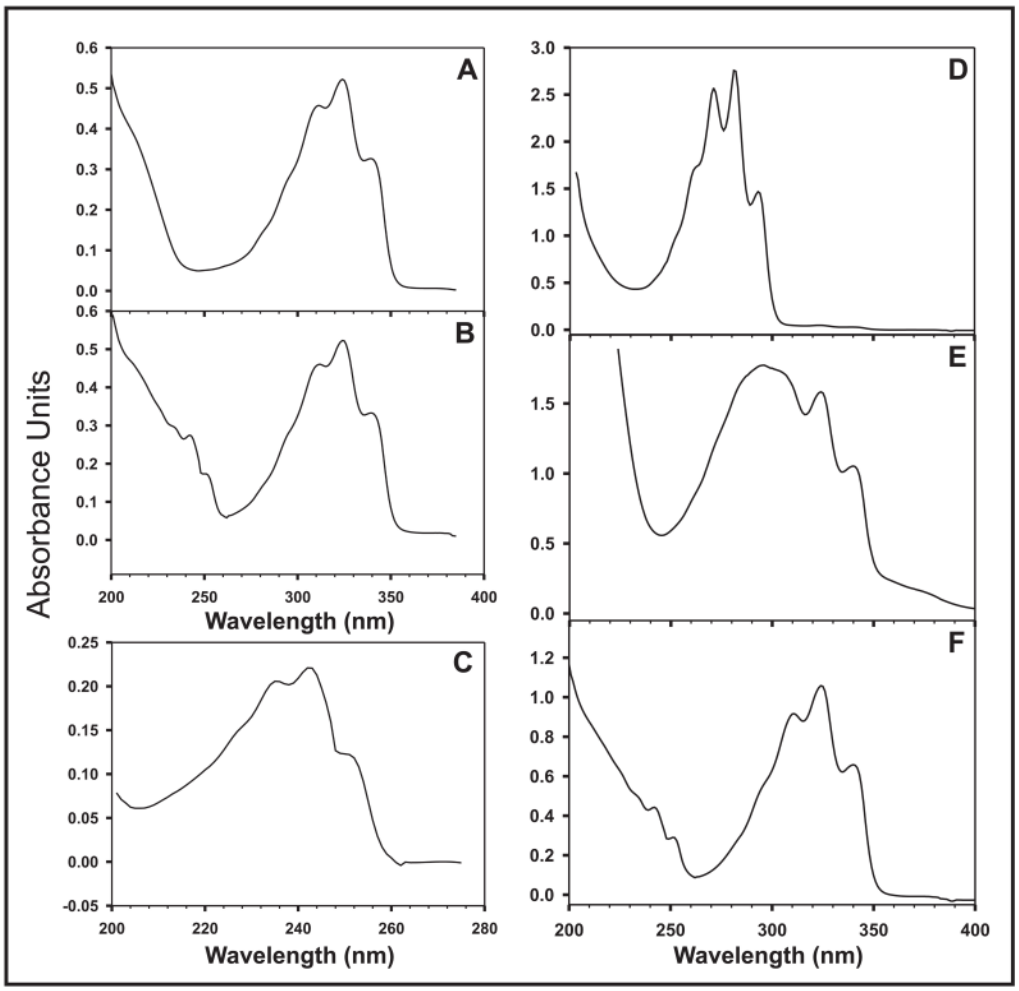


**Fig. 3. Absorption spectra of DHE**

**A.** Pure (~99%) DHE synthesized by an improved method as described in Methods. **B.** Commercially available DHE (Sigma). **C.** Difference spectrum was calculated by subtraction of **(A)** from **(B)**. This spectrum shows the triene impurity alone. *Note*: it was necessary to use absorbance spectra to characterize the impurity, since the emission and excitation spectra determined the impurity was non-fluorescent (not shown). **D.** UV absorbance spectrum of ergosterol acetate. **E.** UV absorbance spectrum taken after 16 h dehydration of ergosterol acetate. **F.** UV absorbance spectrum of the resultant DHE acetate with impurity from the dehydration step.

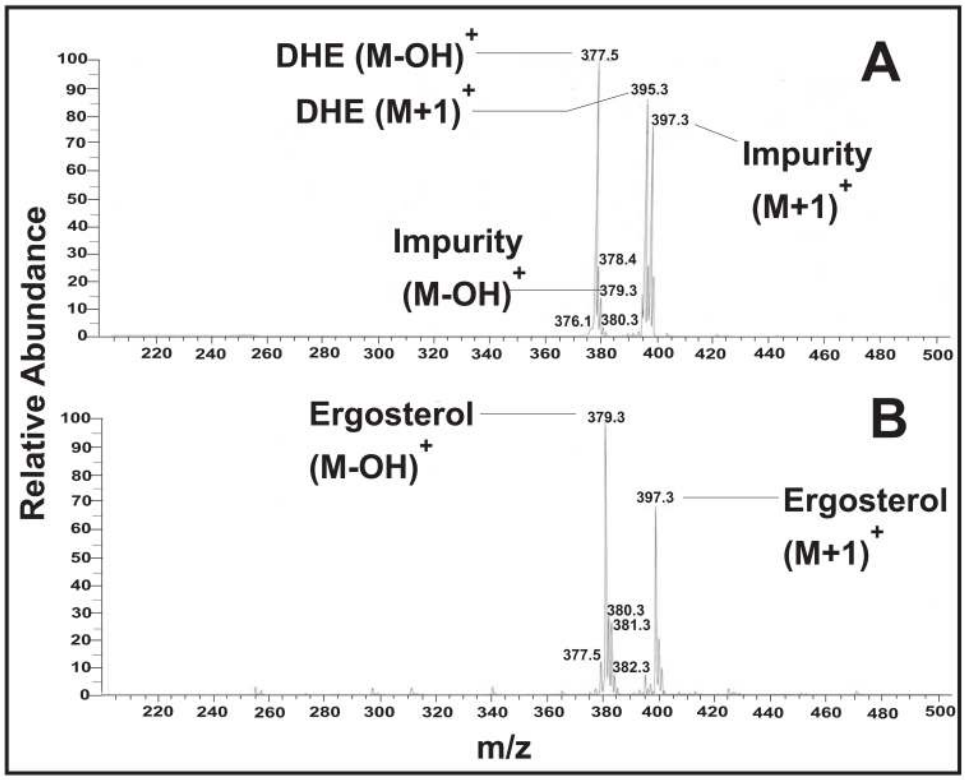


**Fig. 4. Atmospheric pressure chemical ionization (APCI) mass spectra of the DHE and ergosterol**

Mass spectral analysis was performed with a Thermo Finnigan LCQ Deca ion trap liquid chromatograph mass spectrometer (Thermo Finnigan, San Jose, CA) in atmospheric pressure chemical ionization (APCI) ion mode with sample flow rates of 200 μl/min near the quadrupole ion trap mass analyzer involving ultra-high purity helium gas. Samples were brought up in 1 μMolar solutions of equal volumes of MeOH and $H_2O$ where both the methanol and $H_2O$ were HPLC grade Burdick and Jackson (Muskegon, MI) purchased from VWR (Atlanta, GA). **A.** Mass spectrogram of impure DHE (Fig. 2A-C). The daughter ion resulting from the parent ion minus a hydroxyl group was indicated by $(M\text{-}OH)^+$ while plus a proton was indicated by $(M+1)^+$. The impurity was observed as a daughter ion resulting from the parent ion losing a hydroxyl group $(M\text{-}OH)^+$ and gaining a proton $(M+1)^+$. **B.** Mass spectrogram of commercially available ergosterol (99% pure), with the observed $(M+1)^+$ and $(M\text{-}OH)^+$ daughter ions. Note that the ergosterol had the same mass as the triene impurity.

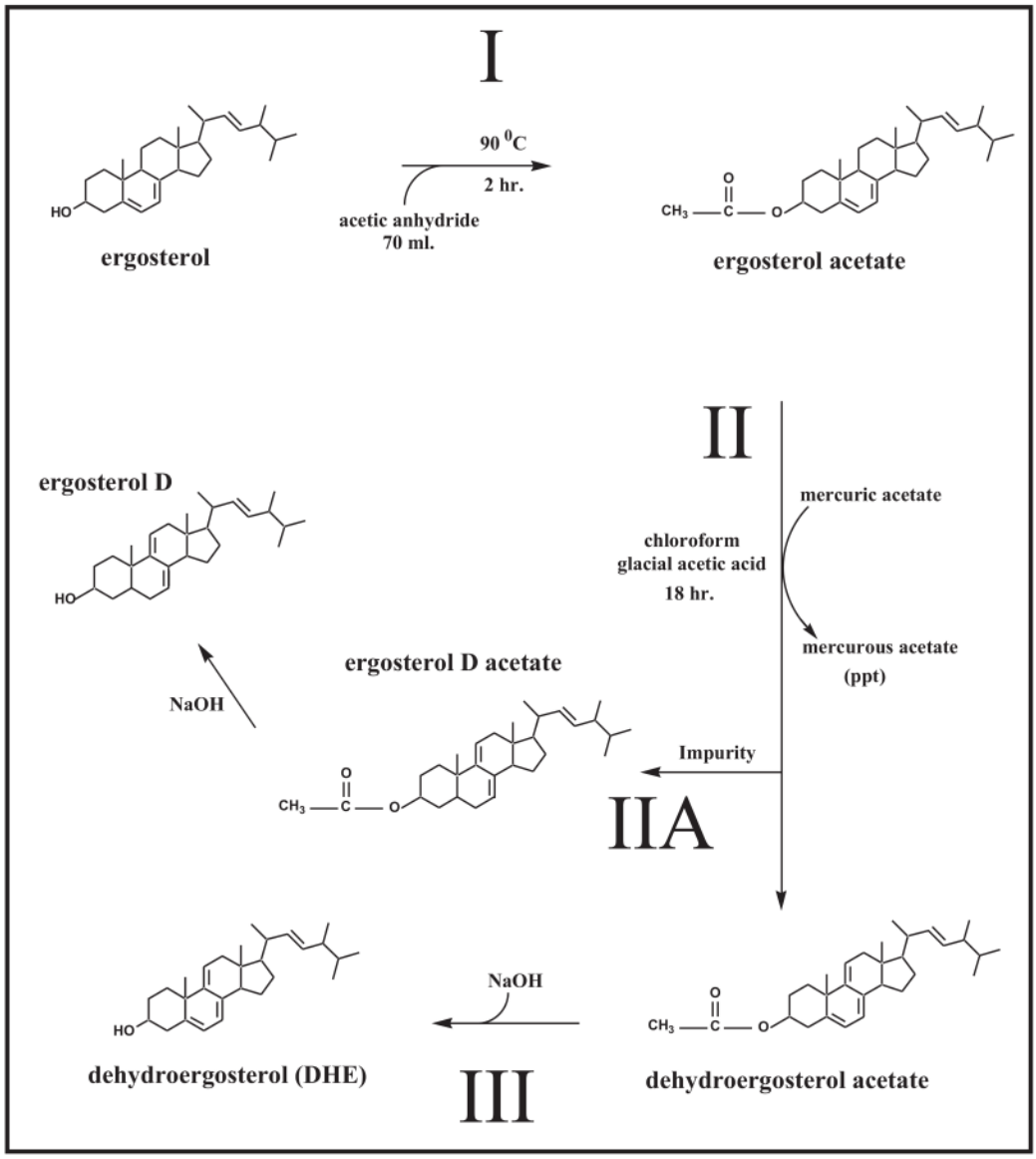


**Fig. 5. General scheme of synthesis of DHE**

Step I is the conversion of ergosterol to ergosterol acetate. Step II is the dehydration of the ergosterol acetate to form a new double bond in the C ring. Step IIA is the competing side reaction which causes formation of the triene impurity in DHE. Note that this triene impurity had the same molecular mass as ergosterol because it was an isomer of ergosterol, *i.e.* ergosterol D. Step III is the saponification of the DHE acetate to yield DHE product.

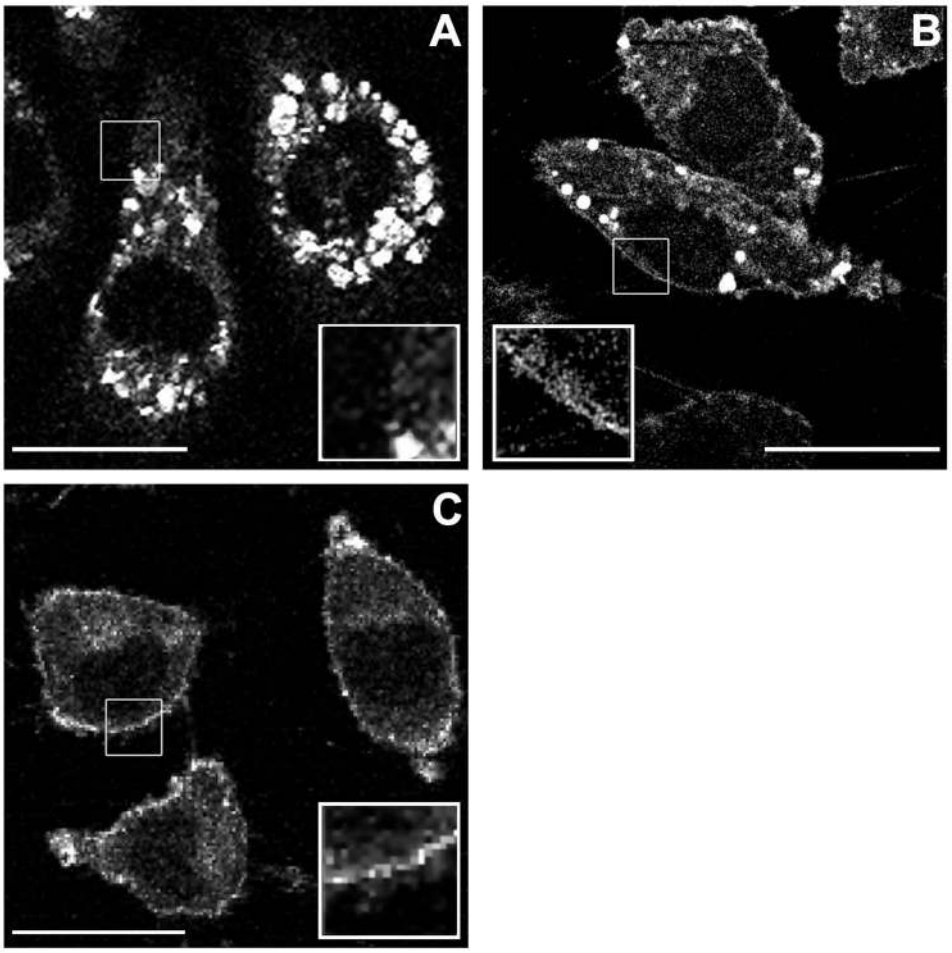


**Fig. 6. Real time multiphoton imaging of DHE in living L-cell fibroblasts**

L-cells were plated onto chambered coverglass incubated with DHE by three different techniques and imaged by multi-photon laser scanning microscopy using a MRC-1024MP system with external non-descanned detection. Excitation occurred at a wavelength of 900 nm using a femto-second modelocked titanium:sapphire laser and the emission was detected through a D400/100 and UV 440LP dichroic filter. **A.** Image of L-cells that were incubated for two days with 20μg DHE from ethanolic stock solution added to 1 mL media (ethanol < 0.5%) wherein large accumulation of crystalline DHE occurred. The high intensities (crystalline DHE) was kept under saturation levels and within the instrumental dynamic range; thus lowering the sensitivity of detection of monomeric DHE within the plasma membrane. **B.** Image of L-cells that were incubated for one day with 20μg DHE in the form of large unilamellar vesicles (65:35 mol % POPC:DHE). **C.** Image of L-cells that were incubated for 45 minutes with 20μg dehydroergosterol methyl-β-cyclodextrin complexes. *Insets:* Regions that included a section of the plasma membrane and outlined in a white rectangle were magnified 2.5X. Bars = 20 μm.